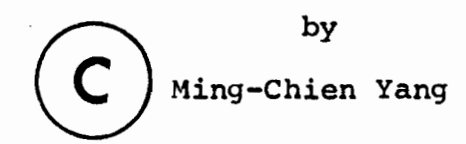
# Development of Minicomputer Control System for Biaxial Extensiometer



Department of Chemical Engineering
McGill University
Montreal, Canada

A thesis submitted to the Faculty of Graduate Studies and Research in partial fulfillment of the requirements for the Degree of Master of Engineering

McGill University Montreal, Canada



#### ABSTRACT

The experimental apparatus for studying biaxial extensional flow that was developed previously by Rhi-Sausi has been modified by adding a minicomputer control system. The main function of this control system is to generate a constant strain rate. By designing an interface circuit, a commercial minicomputer, the Commodore PET, is able to control the inflation of a sheet of molten polymer at a constant strain rate.

With the modification of the apparatus, a new experimental procedure was developed.

Experimental studies of low density polyethylene at  $130^{\circ}$ C were carried out. From the obtained strain-time curves, it is shown that constant strain rate biaxial extensional flow can be generated by the modified rheometer.

The limitations of this prototype and recommendations for future work are also given.

## RESU'IE

L'appareil expérimental développé par J. Rhi-Sausi pour étudier l'extension biaxiale a été modifié par l'addition d'un système de contrôle par micro-ordinateur. La fonction principale du système de contrôle est de générer un taux de déformation constant. Par l'addition d'une interface, un micro-ordinateur commercial de marque "Commodore PET" à la possibilité de contrôler le gonflement d'une feuille de polymère fondu à un taux constant de déformation.

Basé sur les modifications apportées à l'appareil, une nouvelle procédure expérimentale a été developpée. Une étude expérimentale sur un polymère de polyéthylène a basse densité a été effectuée à une température de 130°C. A partir des courbes de déformation versus temps obtenues, il est demontré qu'une extension biaxiale à taux de déformation constant peut être obtenue avec l'appareil ainsi modifié.

Les limitations du prototype ainsi que certaines recommandations pour son utilisation future sont aussi données.

#### ACKNOWLEDGEMENTS

I am sincerely grateful for the help and encouragement from many sources during the completion of this research project.

The most gratitude I would like to express to my supervisor, Professor John M. Dealy, for his advice, encouragement, and help in all aspects of this project.

Many thanks must go to Mr. L.J. Vroomen, Prof. T.J. Boyle and Mr. Bing Huang for their helpful advice in the design of the electronic circuits. I would like to thank Mr. G. Dedik, Mr. G. Tewfic and Mr. W. Hoogendoorn for supplying electronic parts and testing equipment.

Thanks must also go to Dr. V. Tan, for his assistance in the development of experimental techniques.

I like also to express my appreciation to Messrs. A. Krish and W. Greenland for their help in the modification of the apparatus, to Mr. J. Dumont for his repeated assistance in purchasing and obtaining parts.

Among my colleaques, I would like to express my thanks to Mr. P.G. Lafleur for his help in using

MUSIC/Script to prepare this thesis; to Mrs. N.Orbey for her help in photographic methods; to Miss Su-Syin Soong for her consultation in rheology; and to Messrs. E. Chu and A. Kallos for their advice and assistance.

# NOMENCLATURE

# Latin Letters

<b>A</b> .	(1) Surface area, in eq. 2-5
	(2) = $K_G K_A K_M$ , in eq. 4-2
Ao	Initial surface area, in eq. 2-5
A <sub>i</sub>	Surface area in the i-direction, in eq. 1-4
Ap	Piston cross sectional area, in eq. 3-5, 3-12
D ·	Diameter of a meridian on a bubble
đ	Thickness of the sample
do	Initial thickness of the sample
е	A voltage signal
$\mathtt{F_{i}}$	Force component in i-direction
$\mathbf{F}_{\mathbf{T}}$	Tensile force
$\mathbf{F}_{\mathbf{p}}$	Pressure force
G	Controller function
h	The height of a bubble
K	A factor in eq. 3-12
KA	Pitch of the linear actuator
$\kappa_{G}$	Gear ratio
K <sub>M</sub>	The gain of the servoamplifier
k <sub>i</sub>	A constant in eq. 1-8
L	Length

Original length

Pressure

- R Radius of curvature
- r r-component in cylindrical coordinates
- T Tension
- t Time
- V Volume
- v Velocity
- v<sub>i</sub> Velocity component in i-direction
- X Piston displacement
- x Diameter of a meridian on the bubble
- x<sub>O</sub> Initial value of x
- z z-component in cylindrical coordinates

## Greek Letters

- α Total angle of the curvature
- $\beta$  Angle as defined in Fig. 3-7
- Δ Rate-of-deformation tensor
- $\Delta_{ii}$  ij-th element of  $\Delta$
- Δl Elongated length
- ε Strain
- $\epsilon_{h}$  Biaxial extensional strain
- $\varepsilon_i$  Strain in i-direction
- ¿ Strain rate
- $\eta_0$  Zero shear viscosity
- n<sub>b</sub><sup>+</sup> Biaxial stress growth function
- nb Biaxial extensional viscosity
- $\theta$   $\theta$ -component in cylindrical coordinate
- $\lambda$  Elongation ratio

p Density

o<sub>b</sub> Biaxial stress

<u>τ</u> Stress tnsor

 $\tau_{ij}$  The ij-th element of the stress tensor

ω Angular velocity

# TABLE OF CONTENT

Abstract	i
Resume	ii
Acknowledgement	iii
Nomenclature	iv
Introduction	1
Ch. 1 General Background	3
1-1. Definitions	3
1-1-1. Strain and Strain rate	3
1-1-2. Stress	4
1-1-3. The Rate-of-deformation Tensor	5
1-2. Basic Assumptions	7
(1) The fluid is a continuum	7
(2) The material is incompressible	8
(3) The fluid is isotropic at rest	8
1-3. Biaxial Extensional Flow	8
1-3-1. Extensional Flow	8
1-3-2. Biaxial Extensional FLow	10
1-3-3. The Material Function	12
Ch. 2. Experimental Mehtods Reported	
in the Literature	14
2-1. The Use of Pressure Grips	14
2-2. The Use of Rotary Clamps	14
2.2 Tubulastal Guusaa Mlaa	1.5

2-4. Sheet Inflation	16
Ch. 3. The McGill Biaxial Extensiometer	21
3-1. The First Prototype	21
3-2. The Second Prototype	24
3-3. Detailed Description of the System	24
A. The Mobile Chamber	26
B. The Fixed Chamber	29
C. The Clamping Ring	29
D. The Control System	32
E. The Recording System	32
3-4. Remaining Problems of the Second Prototype	33
Ch. 4. The Digital Control System	38
4-1. Control Strategies	38
4-1-1. Analog Control versus Digital Control	. 38
4-1-2. Direct Digital Control versus	
Supervisory Computer Control	39
4-1-3. The Selection of the Controller Function	41
4-1-4. Summary	46
4-2. Hardware Description	48
4-2-1. The Digital Computer	48
4-2-2. The Interface Circuit	48
4-3. Description of the Software	52
4-3-1. The Program "TEST"	52
4-3-2. The Program "TST1"	56

Ch. 5. Day and any half Day and June	,
Ch. 5. Experimental Procedure58	
5-1. Sample Preparation58	}
5-2. Loading the Instrument58	}
5-3. Operation of the Extensiometer60	)
5-3-1. Switching 61	1
5-3-2. Program-Loading 63	3
5-3-3. Program-Running 63	3
5-3-4. Unloading the Extensiometer 64	ļ
5-4. The Adjustment and Calibration	
of the Control System64	ļ
5-4-1. The Calibration of the Pressure Transducer 64	ļ
5-4-2. The Zeroing of the Position Reading 67	7
5-4-3. The Calibration of the D/A Output 67	7
<b>2</b>	
Ch. 6. Determination of the Material Function70	)
6-1. Data Analysis Procedure70	C
6-2. The Determination of the Strain	2
6-3. The Calculation of the Stress	3
6-4. The Calculation of the Material Function7	5
6-5. Discussion of Experimental Results	5
Ch. 7. Experience During Apparatus Modification78	3
7-1. Designing the Hardware78	3
7-2. Designing the Software8	0
7-3. Development of Experimental Techniques8	1
7-4. Operation of the Extensiometer8	2
7-4-1 Photography 8	2

7-4-2. Pressure Balancing Before an Experiment	82
Ch. 8. Summary and Recommendations	
8-1. Summary	84
8-1-1. The Hardware Development	84
8-1-2. The Software Development	84
8-1-3. The Development of Experiment Technique	84
8-1-4. Demonstration of the Extensiometer	85
8-2. Recommendations	85
8-2-1. Improvement of the Extensiometer	85
8-2-2. Improvement of the Experiment Technique	86
References	87
Appendix A. Programs and Circuit Diagram	89
Appendix B. Experimental Results	95
Appendix C. Glossary of terms1	08

#### INTRODUCTION

In contrast with shear flows, extensional flows were neglected for quite a long time, although these are the predominant flow patterns in certain polymer processing operations such as spinning, blow molding, film blowing, and so on, and that is why there is an increasing interest in these flows. Data on extensional flows are needed for testing models of the rheological behavior of polymer melts in this type of flow.

To serve as a basis for testing the various models existing at the present time, several material functions have been defined. The material function of steady biaxial extensional flow is the biaxial extensional stress growth function, which is the object to be determined by the experimental technique developed in this reseach.

In studying biaxial extensional flow, however, it is very difficult to generate uniform deformation of the material at a controlled strain rate. The sheet inflation technique, which has been used previously to study rubber and very high viscosity melts, has been adopted in spite of the difficulty of generating a constant strain rate. By developing a digital control system, this long-time problem has been solved. An empirical equation for generating

constant strain rate is found and curves of the biaxial extensional stress growth function at several strain rates have been obtained.

A general theoretical description of biaxial extensional flow is given in chapter 1 to provide a background for study. In chapter 2 the previous research work on biaxial extension is reviewed, including contributions as well as limitations. In chapter 3, the extensiometer that had been constructed in McGill is described, and the defects of this apparatus are discussed.

The main improvement made in this project, the development of the digital control system, is described in chapter 4. In chapter 5, a new experimental procedure is given. The analyzing of data and the computation of the material function are given in chapter 6. The experiences of developing this new technique are described in chapter 7, and the conclusions and recommendations are presented in the last chapter.

In appendix A, the program listings and the circuit diagram of the interface circuit are presented. All the experimental results are given in appendix B. A glossary of terms used is given in appendix C.

#### CH. 1 GENERAL BACKGROUND

#### 1-1. Definitions:

or

## 1-1-1. Strain and Strain rate:

For an elastic body, such as a rubber band, the extent of the deformation is described by the ratio of the change of length,  $\Delta \ell$ , to the original length,  $\ell_0$ 

$$\varepsilon = \frac{\Delta \ell}{\ell_0} \tag{1-1}$$

This ratio is called the Cauchy Strain.

But, unlike a rubber, for which the recovery of the stretching is complete, in the case of a viscoelastic liquid, when the force is removed after stretching the material cannot retract back to its original length; in other words, the material has a "fading memory". Hence, it is meaningless to compare the stretched length with the original length. An alternative measure of strain is used in this case:

$$d\varepsilon = \frac{d\ell}{\ell}$$

$$\varepsilon = \int_{\ell}^{\ell} \frac{d\ell}{\ell} = \ln \frac{\ell}{\ell}$$
(1-2)

4

This is called the <u>Hencky strain</u> and is the definition used in this thesis.

The strain rate is simply the derivative of the strain with respective to the time:

$$\dot{\varepsilon} = \frac{d\varepsilon}{dt} = \frac{d \ln \ell}{dt} \tag{1-3}$$

## 1-1-2. Stress:

This term is a useful concept to describe the momentum transfer in a material matrix. The stress is defined as the force exerted per unit surface area, and its unit in the SI system is newton per square meter or pascal. Considering a control volume, the forces acting on the mass in the volume can be attributed to two different types of sources: the body forces, such as the gravity, and the surface forces, which are associated with deformation and motion. The stress describes only the latter. In a 3-dimensional coordinate system, Cartesian coordinates for example, the force can be resolved into 3 components, while the faces of the control volume, defined by their normals, are also in 3 directions; thus there are nine possible combinations of the direction-related quotient, the stress:

$$\tau_{ij} = dF_i / dA_i \qquad (1-4)$$

These quantities are the nine components of a tensor,  $\underline{\tau}$ ,

which is expressed below :

$$\underline{\tau} = \begin{pmatrix} \tau_{11} & \tau_{12} & \tau_{13} \\ \tau_{21} & \tau_{22} & \tau_{23} \\ \tau_{31} & \tau_{32} & \tau_{33} \end{pmatrix}$$
 (1-5)

Those components for which i=j, are called "normal stresses", and the rest are "shear stresses".

Although there is an alternative sign convention, the one used here is that if both the directions of the force and the normal of the surface are in their positive directions, the stress is positive. Thus a positive normal stress represents a tension.

In the absence of body couples, from the principle of moment of momentum (the net torque on a fluid element is equal to the rate of change of its angular momentum), the stress tensor can be shown to be a symmetrical tensor.

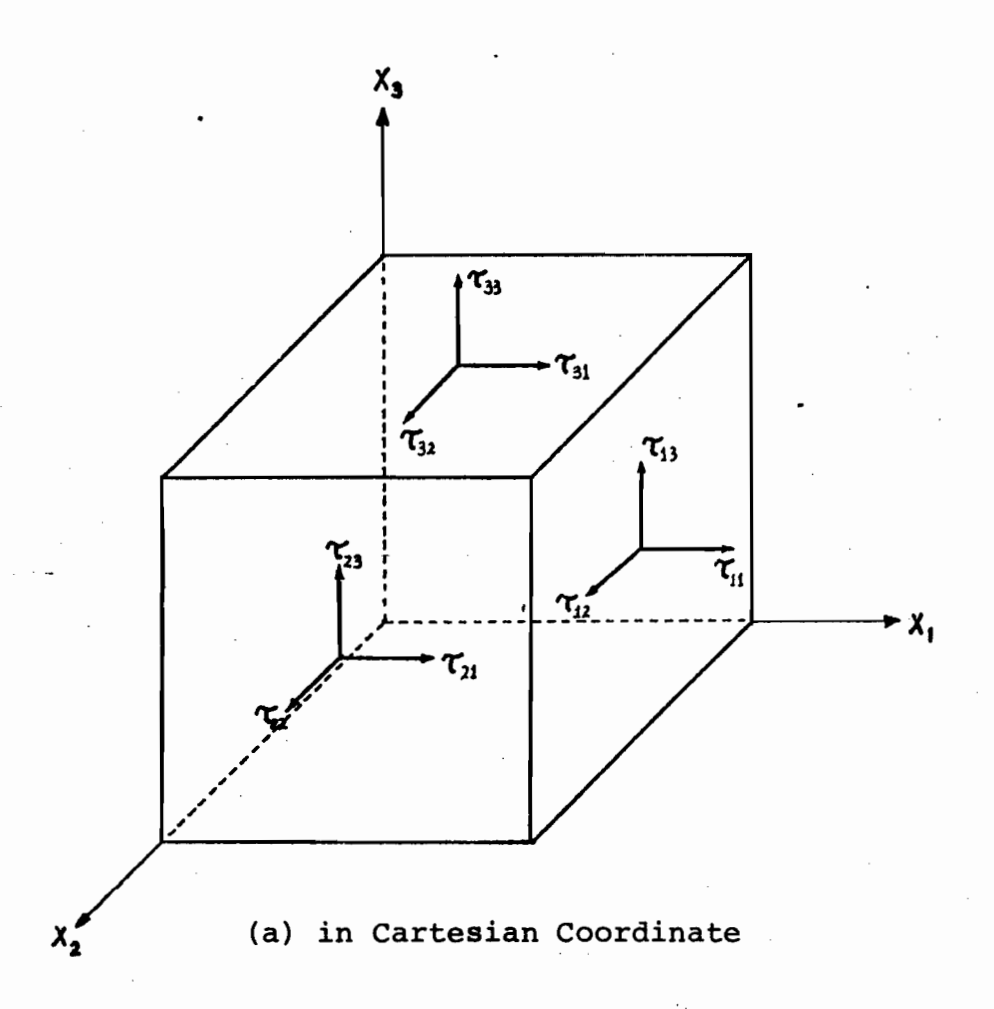
## 1-1-3. The Rate-of-Deformation Tensor:

The rate-of-deformation tensor is defined as follows,

$$\underline{\Lambda} = \nabla \overrightarrow{\mathbf{v}} + (\nabla \overrightarrow{\mathbf{v}})^{\mathbf{T}} \tag{1-6}$$

In Cartesian coordinate, its components are given as follows:

$$\Delta_{ij} = \frac{\partial v_i}{\partial x_j} + \frac{\partial v_j}{\partial x_i}$$
 (1-7)



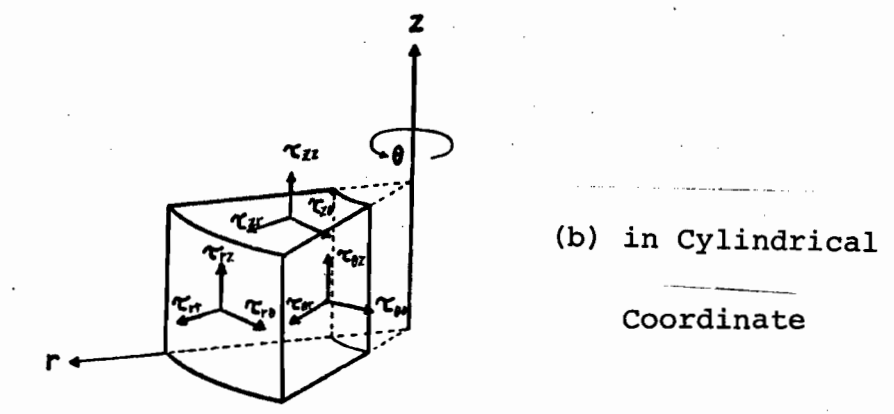


Fig. 1-1. The Stress Tensor

and in cylindrical coordinates, they are expressed as follows .

$$\Delta_{\theta\theta} = 2\left(\frac{1}{r}\frac{\partial v_{\theta}}{\partial \theta} + \frac{v_{r}}{r}\right)$$

$$\Delta_{rr} = 2\frac{\partial v_{r}}{\partial r}$$

$$\Delta_{zz} = 2\frac{\partial v_{z}}{\partial z}$$

$$\Delta_{r\theta} = \Delta_{\theta r} = r\frac{\partial}{\partial r}(\frac{v_{\theta}}{r}) + \frac{1}{r}\frac{\partial v_{r}}{\partial \theta}$$

$$\Delta_{zr} = \Delta_{rz} = \frac{\partial v_{z}}{\partial r} + \frac{\partial v_{r}}{\partial z}$$

$$\Delta_{\theta z} = \Delta_{z\theta} = \frac{\partial v_{\theta}}{\partial z} + \frac{1}{r}\frac{\partial v_{z}}{\partial \theta}$$
(1-7a)

This symmetric tensor describes the relative motion of neighboring fluid particles with respect to one another. It is worth mentioning that the stress tensor components  $\tau_{ij}$  depend only on  $\Delta_{ij}$  for a wide class of materials, so that this tensor provides the essential relationship between the stress and the velocity field.

#### 1-2. Basic Assumptions:

Three assumptions are made to simplify description of the complex flow behavior of polymer melts:

#### (1) The fluid is a continuum.

A continuum is a region of space through which properties such as temperature, pressure, density and velocity may vary in a continuous manner. For the analyzing of the fluid flow, this assumption can be regarded

as true, since in the smallest distance of practical significance, an adequate number of molecules can be found, such that the flow behavior can be described by the average properties over this distance.

(2) The material is incompressible.

Under the condition of constant temperature and low pressure, this assumption may be considered as true, because the change in density is negligible.

(3) The fluid is isotropic at rest.

In an isotropic material, all properties are independent of orientation. In practice this assumption is generally true for polymer melts, except for "liquid crystal" systems like certain polyesters.

## 1-3. Biaxial Extensional Flow:

#### 1-3-1. Extensional Flows:

An extensional flow is defined as a flow with a velocity field given by

$$v_{i} = k_{i} \cdot x_{i} \tag{1-8}$$

where the subscript i represents the i-direction of the

Cartesian coordinate. In steady extension, these factors k<sub>i</sub> are constants.

Since the fluid has been assumed incompressible, from the continuity equation,

$$\nabla \cdot \overset{\rightarrow}{\mathbf{v}} = \frac{\partial \mathbf{v}_1}{\partial \mathbf{x}_1} + \frac{\partial \mathbf{v}_2}{\partial \mathbf{x}_2} + \frac{\partial \mathbf{v}_3}{\partial \mathbf{x}_3} = 0 \tag{1-9}$$

thus  $\Sigma k_i = 0$  (1-10)

Eq. 1-8 can be rewritten as

$$k_{i} = \frac{v_{i}}{x_{i}}$$

$$= \frac{1}{x_{i}} \frac{dx_{i}}{dt}$$

$$= \frac{d \ln x_{i}}{dt}$$
(1-11)

which is coincident with eq. 1-3, the definition of the strain rate,  $\dot{\epsilon}_i$ , so that  $k_i$  is the strain rate and will be replaced by  $\dot{\epsilon}_i$  hereafter.

From the definition of  $\underline{\Delta}$ , the rate-of-deformation tensor is given as :

$$\underline{\Delta} = \begin{bmatrix} 2\mathring{\epsilon}_1 & 0 & 0 \\ 0 & 2\mathring{\epsilon}_2 & 0 \\ 0 & 0 & 2\mathring{\epsilon}_3 \end{bmatrix}$$
 (1-12)

From eq. 1-8, all the terms  $\frac{\partial v_i}{\partial x_j}$ , i=j, do not exist in

extensional flow, thus there is no shearing effect in the flow, and hence, no shear stress exists; in other words, this flow is shearfree. The stress tensor is expressed as

$$\underline{\tau} = \begin{bmatrix} \tau_{11} & 0 & 0 \\ 0 & \tau_{22} & 0 \\ 0 & 0 & \tau_{33} \end{bmatrix}$$
 (1-13)

## 1-3-2. Biaxial extensional flow:

In this type of extensional flow, the strain rate is equal in two orthogonal directions, i.e.

$$\dot{\varepsilon}_1 = \dot{\varepsilon}_2 = \dot{\varepsilon}_h \tag{1-14}$$

and from eq. 1-10,

$$\dot{\varepsilon}_3 = -2\dot{\varepsilon}_b$$
 (1-15)

Here  $\dot{\epsilon}_b$  is the principal rate of biaxial extension.

Practically it is more convenient to describe this flow in cylindrical coordinates:

$$v_{r} = \cos\theta \cdot v_{1} + \sin\theta \cdot v_{2}$$

$$= \dot{\varepsilon}_{b}(x_{1} \cdot \cos\theta + x_{2} \cdot \sin\theta)$$

$$= \dot{\varepsilon}_{b}(r \cdot \cos^{2}\theta + r \cdot \sin^{2}\theta)$$

$$= \dot{\varepsilon}_{b}r \qquad (1-16)$$

$$v_{\theta} = -\sin\theta \cdot v_{1} + \cos\theta \cdot v_{2}$$

$$= \dot{\varepsilon}_{b} (x_{1} \cdot \sin\theta + x_{2} \cdot \cos\theta)$$

$$= \dot{\varepsilon}_{b} (-r \cdot \cos\theta \sin\theta + r \cdot \sin\theta \cos\theta)$$

$$= 0$$
(1-17)

$$v_{z} = -2\dot{\varepsilon}_{b}x$$

$$= -2\dot{\varepsilon}_{b}z$$
(1-18)

and the rate-of-deformation tensor, from eq. 1-7a, is expressed as

$$\underline{\Lambda} = \begin{bmatrix} 2\dot{\varepsilon}_{\mathbf{b}} & 0 & 0\\ 0 & 2\dot{\varepsilon}_{\mathbf{b}} & 0\\ 0 & 0 & -4\dot{\varepsilon}_{\mathbf{b}} \end{bmatrix} = 2\dot{\varepsilon}_{\mathbf{b}} \begin{bmatrix} 1 & 0 & 0\\ 0 & 1 & 0\\ 0 & 0 & -2 \end{bmatrix}$$
 (1-19)

If the gravity effect is neglected, from the equation of motion in terms of Cartesian coordinates, it is easy to show that, since

$$\rho \frac{\overrightarrow{Dv}}{Dt} = \nabla \cdot \underline{\tau}$$

$$2\rho \dot{\epsilon}_{b} v_{1} = \frac{\partial \tau_{11}}{\partial x_{1}} \qquad \tau_{11} = \rho \dot{\epsilon}_{b}^{2} x_{1}^{2} = \rho v_{1}^{2} \qquad (1-20a)$$

$$2\rho \dot{\epsilon}_{b} v_{2} = \frac{\partial \tau_{22}}{\partial x_{2}} \qquad \tau_{22} = \rho \dot{\epsilon}_{b}^{2} x_{2}^{2} = \rho v_{2}^{2} \qquad (1-20b)$$

$$-4\rho \dot{\epsilon}_{b} v_{3} = \frac{\partial \tau_{33}}{\partial x_{3}} \qquad \tau_{33} = 4\rho \dot{\epsilon}_{b}^{2} x_{3}^{2} = \rho v_{3}^{2} \qquad (1-20c)$$

Because the material has been assumed isotropic,  $\mathbf{v}_1$  and  $\mathbf{v}_2$  must be the same, therefore,

$$\tau_{11} = \tau_{22}$$
 (1-21)

By transforming eq. 1-21 into cylindrical coordinate, the following result is obtained,

$$\tau_{rr} = \tau_{\theta\theta} \tag{1-21a}$$

Thus the stress tensor  $\tau$  is:

$$\underline{\tau} = \begin{pmatrix} \tau_{rr} & 0 & 0 \\ 0 & \tau_{rr} & 0 \\ 0 & 0 & \tau_{zz} \end{pmatrix}$$
 (1-22)

However, only the stress difference  $\tau_{rr} - \tau_{zz}$  is of rheological significance, and it will be written as:

$$\sigma_{\mathbf{b}} = \tau_{\mathbf{rr}} - \tau_{\mathbf{zz}} \tag{1-23}$$

# 1-3-3. The material function:

For an incompressible non-Newtonian fluid, it is impossible to obtain the velocity distribution and the stresses without knowing the correlation between these two terms. To solve this problem, several models have been proposed, but usually they have several constants to be determined. Material functions provide the basis for the determination of these constants.

In steady biaxial extensional flow, the material function is called the biaxial extensional stress growth function.

$$\eta_{\mathbf{b}}^{+}(\hat{\epsilon}_{\mathbf{b}}, t) \equiv \frac{\sigma_{\mathbf{b}}(t)}{\hat{\epsilon}_{\mathbf{b}}}$$
 (1-24)

At long times, it is believed that this function will reach a steady state value, called the extensional viscosity.

$$\lim_{t \to \infty} \eta_b^+ = \eta_b(\dot{\varepsilon}_b) \tag{1-25}$$

When  $\epsilon_{\rm b}$  is very small, the biaxial extensional stress growth function becomes equal to six times the stress growth function for shear.

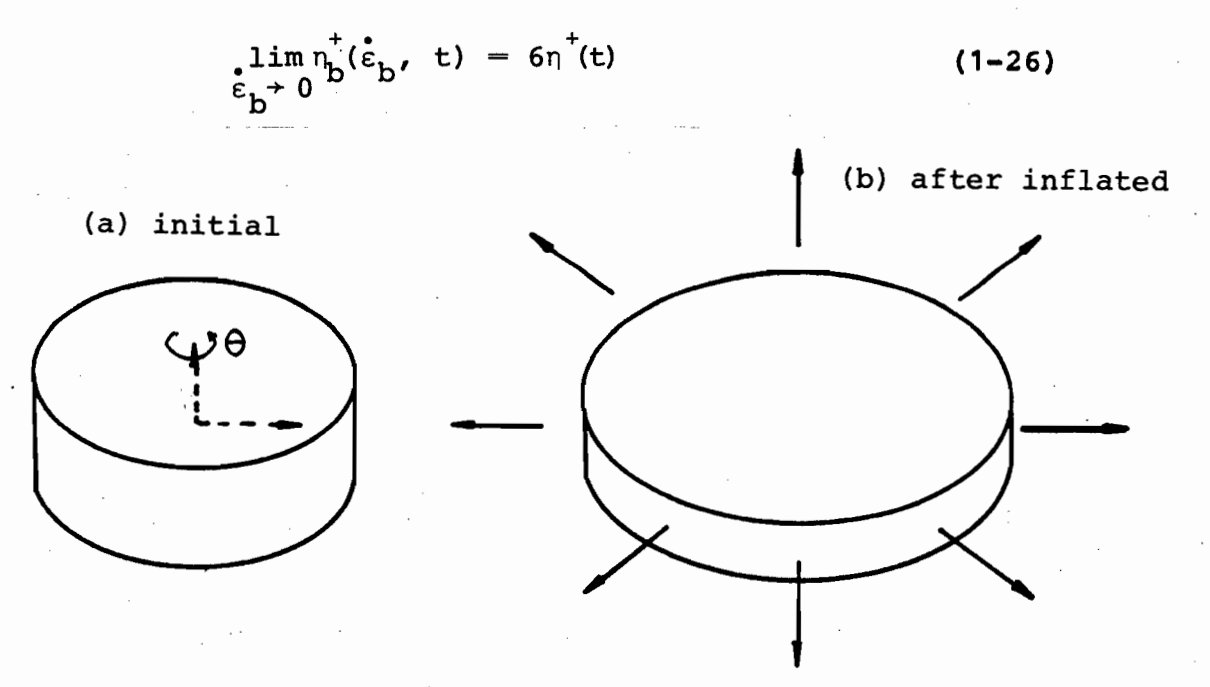


Fig. 1-2. Equal Biaxial Extension

#### CH.2. EXPERIMENTAL METHODS REPORTED IN THE LITERATURE

The generation of biaxial extensional flow is much more difficult than that of uniaxial extensional flow. However, descriptions of several methods that have been employed can be found in the literature.

## 2-1. The Use of Pressure Grips :

Thomas and Cleeremen (2.1) clamped a square or circular sheet around its periphery, and provided a mechanism to move the clamps outward along radial lines. However, this technique is useful only for rubbers and glassy polymers and is not practical for polymer melts.

#### 2-2. The Use of Rotary Clamps:

Farber (2.2) built a prototype based on a pair of flexible hoops which could be rotated around their own cores, but problems were encountered: substantial friction was introduced by the guide grooves for the hoops and the drive gears; in addition, the rotation of the hoops was interfered with by the polymer collected at the outer hoop perimeter.

A more successful prototype has been built by Meissner

et al. (2.3). Eight rotary clamps are arranged in a circle, and eight automated scissors cut the sheet of molten polymer between the clamps at frequent intervals. This cutting produces eight strips of polymer which can be wound up on rollers. Although periodic fluctuations in the measured tensile force is introduced by the cutting, it is reported that meaningful values of time-dependent stress can be determined from the experimental data. This technique has been used so far only with polyisobutylene at room temperature, but work is continuing to extend it to the study of molten polymers.

## 2-3. Lubricated Squeeze Flow:

The use of "lubricated squeeze flow" to generate biaxial extension has been suggested by Stevenson (2.4). Although the flow of a melt squeezed between two unlubricated parallel flat plates is not a biaxial extensional deformation, the use of lubricant, a relatively inviscid liquid, will prevent contact between the melt and the plates so that a biaxial extensional flow is generated, if the thickness of the lubricant is uniform.

For a constant strain rate,  $\dot{\epsilon}_b$ , the velocity of the moving plate is

$$v_z = -2\dot{\varepsilon}_b z = \frac{dz}{dt}$$
 (2-1)

Then the plate spacing is

$$z = z_0 e^{-2\hat{\epsilon}} b^{t}$$
 (2-2)

and the strain is

$$\varepsilon_{\rm b} = \frac{1}{2} \ln \frac{z}{z_0} \tag{2-3}$$

Since the material is assumed to be incompressible, the volume, V, is given by

$$V = \pi r_0^2 h_0 ag{2-4}$$

and the stress is

$$\sigma_{\mathbf{b}} = \frac{\mathbf{F}}{\mathbf{A}} = \frac{\mathbf{F}\mathbf{z}}{\mathbf{A}_0 \mathbf{Z}_0} \tag{2-5}$$

where F = the force exerted by the squeezing

A = the contact area of melt with the plate

This method has been used by Macosko et al (2.5) for measurements at room temperature.

# 2-4. Sheet Inflation:

The most popular technique to date has been the bubble (or sheet) inflation method. A sheet of the melt is inflated into a bubble by applying pressure on one side, and

a uniform biaxial extension will occur in the region near the pole of the bubble. This method was first developed in the study of rubber elasticity by Treloar (2.6).

Denson and Gallo (2.7) employed the sheet inflation technique to generate biaxial extensional flow. A sheet of polyisobutylene was clamped between two flat plates. A hole of diameter 2.54 cm was machined in the center of the upper plate for the swelling of the bubble. A smaller hole in the center of the lower plate was fitted with a tube which was connected to a compressed nitrogen tank. Two valves were installed on the pressure tube, and a tee junction, located in between, was connected to a manometer to measure the After the pressure was adjusted to a certain value, the valve to the nitrogen supply was closed, and the valve to the sample was opened, inflating the sheet. The height of the bubble was measured by a cathetometer. The biaxial extensional viscosity was found to decrease with strain rate according to a power law, and to decrease with molecular weight. It was concluded that more accurate information could be obtained by restricting strain measurement to a small circular area near the pole of the bubble where uniform biaxial extension exists.

The above technique was later improved by Joye, Poehlein, and Denson (2.8). Their improvements included 1, the use of cinematographic analysis of the rate of separation of circles on the surface of the samples in the

region near the pole; 2, film records of the bubble shape, and; 3, the use of a pressure transducer. The bubble expanded under constant tension. This requirement was achieved by using a so-called "constant mass" method to generate pressure according to the relationship:

$$PR^2h = \frac{P(a^2 + h^2)^2}{4h} = constant$$
 (2-6)

This "constant mass" method was the injection of a fixed mass of nitrogen at a predetermined pressure and temperature into a close volume beneath that part of material to be deformed. The volume of gas was determined by a trial and error procedure.

The biaxial extensional viscosity for the material was found to decrease as the strain rate increases, but at low strain rate, the extensional stress growth function disagreed with the value predicted from stress relaxation data and linear viscoelasticity theory. Predictions of several constitutive equations were presented, but no attempt was made to compare them with the experimental data.

Maerker and Schowalter (2.9) attempted to obtain a constant strain rate by regulating gas flow to the inflating bubble. In addition to local deformation measurement, the polyisobutylene they studied had lower viscosity than any other material used in biaxial experiments. They concluded that the gas inflation method is limited to materials with

zero shear viscosity above 10 Pa.s.

De Vries and Bonnebat (2.10) used an elaborate apparatus to generate a constant strain rate flow. A caliper-like device with its two tips "welded" ultrasonically to the sample surface near the pole acts as a strain transducer, and the signal generated is used to operate a feedback control system which is regulating the flow of air into the inflating sheet.

Hoover and Tock (2.11) used a displacement transducer with its shaft directly in contact with the top of the bubble to monitor the deformation. However, the direct measurement of strain is not so straightforward when the material studied is a melt.

All the above devices were designed for measurement at ambient temperature with a gas as the inflation medium. Thus operation at elevated temperatures was not possible, and only high viscosity materials could be studied, as there was no support for the sample prior to the inflation. Furthermore, because of the compressibility of the gas, direct control of the inflation rate was not possible.

Denson and Hylton (2.12) used a liquid inflation medium to study the extension of several very high viscosity materials, which is worth mentioning. A signal proportional to the stress was produced by a pressure signal and an

empirical relationship between the sample thickness, the radius of curvature, and the inflated bubble volume. This signal was used as the set point to control the sheet inflation process. However, the flow generated is actually a planer extension since a rectangular sheet was inflated. Although they had done experiments in biaxial extension, the results are not reported.

Dealy and Rhi-Sausi (2.13) built an apparatus using oil as the inflation medium, which will be described in the next chapter.

A complete table given by Petrie (2.14) summarizes work on biaxial extensional flow.

#### CH. 3. THE MCGILL BIAXIAL EXTENSIOMETER

#### 3-1. The First Prototype:

To explore the biaxial extensional flow behavior of polymer melts at high temperature, a prototype was built by Rhi-Sausi according to the design of Farber, as shown in Α flat, disk-shaped Fig.3-1. sample was clamped horizontally between two chambers. These two chambers were both filled with silicone oil which served as the heating medium and equalized the hydrostatic head. Tubular cartridge heaters were located in the lower chamber wall. These two chambers were covered by an insulation jacket. The sample holder consisted of a fixed ring and a movable ring keeping the sample in between. A pressure transducer was installed in the holder. To keep the polymer melt from flowing out of the ring there was a coolant flow channel in the holder. Observations and photographs were made possible by 4 equally spaced windows located on the upper chamber wall.

The sample was inflated by raising the lower chamber pressure, which was done by the displacement of a piston located in a cylinder mounted on the side of the lower chamber wall. The piston was driven by a servo motor through a linear actuator. The displacement of the piston as a function of time followed an idealized model of

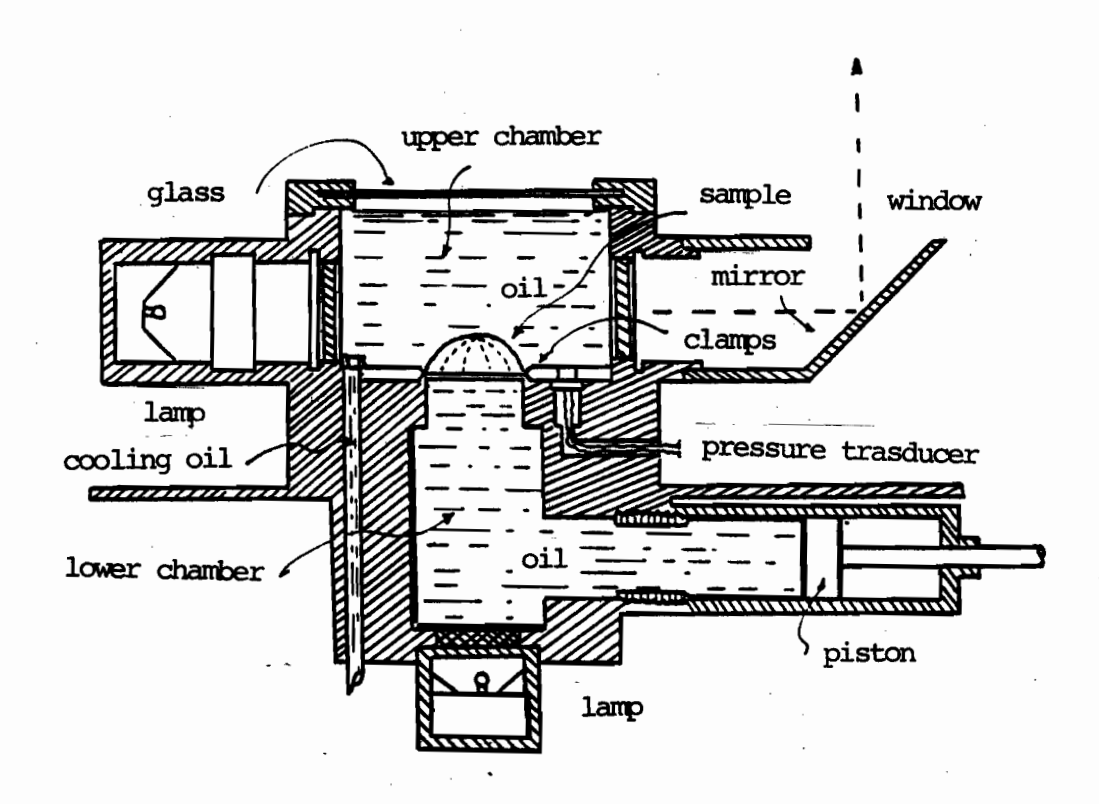


Fig. 3-1. First Prototype

spherical bubble growth, and this function was generated by an analog computer.

After several preliminary tests, the following main problems were encountered:

- 1. Air was trapped under the sample and could not be removed.
- 2. Undesired deformation of the sample, caused by the oil expansion, started before the initiation of the experiment.
- 3. Non-uniformity of the temperature was caused by the water cooling channels.
- 4. Difficulty in controlling the inflation was found due to the short piston displacement, which was required for the complete inflation.
- 5. Difficulty in handling the sample was caused by its large diameter.
- 6. Insufficiency of the heating elements due to heat losses through the upper chamber.
- 7. Operation of the equipment was very complex.

After several unsuccessful attempts to solve the above problems, this model was abandoned, and the second prototype was designed and built by Rhi-Sausi (3.1).

## 3-2. The Second Prototype

To avoid the problems caused by air trapped under the sample, the sample was installed vertically in the new design. As shown in Fig. 3-2, there were two cylindrical chambers, fixed and mobile, mounted horizontally with a sample clamping ring in between. Silicone oil was pumped into these two chambers and heated up to the testing temperature, as in the first prototype. The pressure difference was generated by the displacement of a piston mounted on one end of the fixed chamber. Photographs could be taken through the windows at the end and on the sides of the mobile chambers.

The piston displacement function followed an ideal model, as in the first prototype. The whole system will be described in detail in the next section.

A number of experiments were carried out by Rhi-Sausi and the stress growth function was determined. However, there still remained several problems to be solved, and these will be discussed at the end of this chapter.

# 3-3. The Detailed Description of the System:

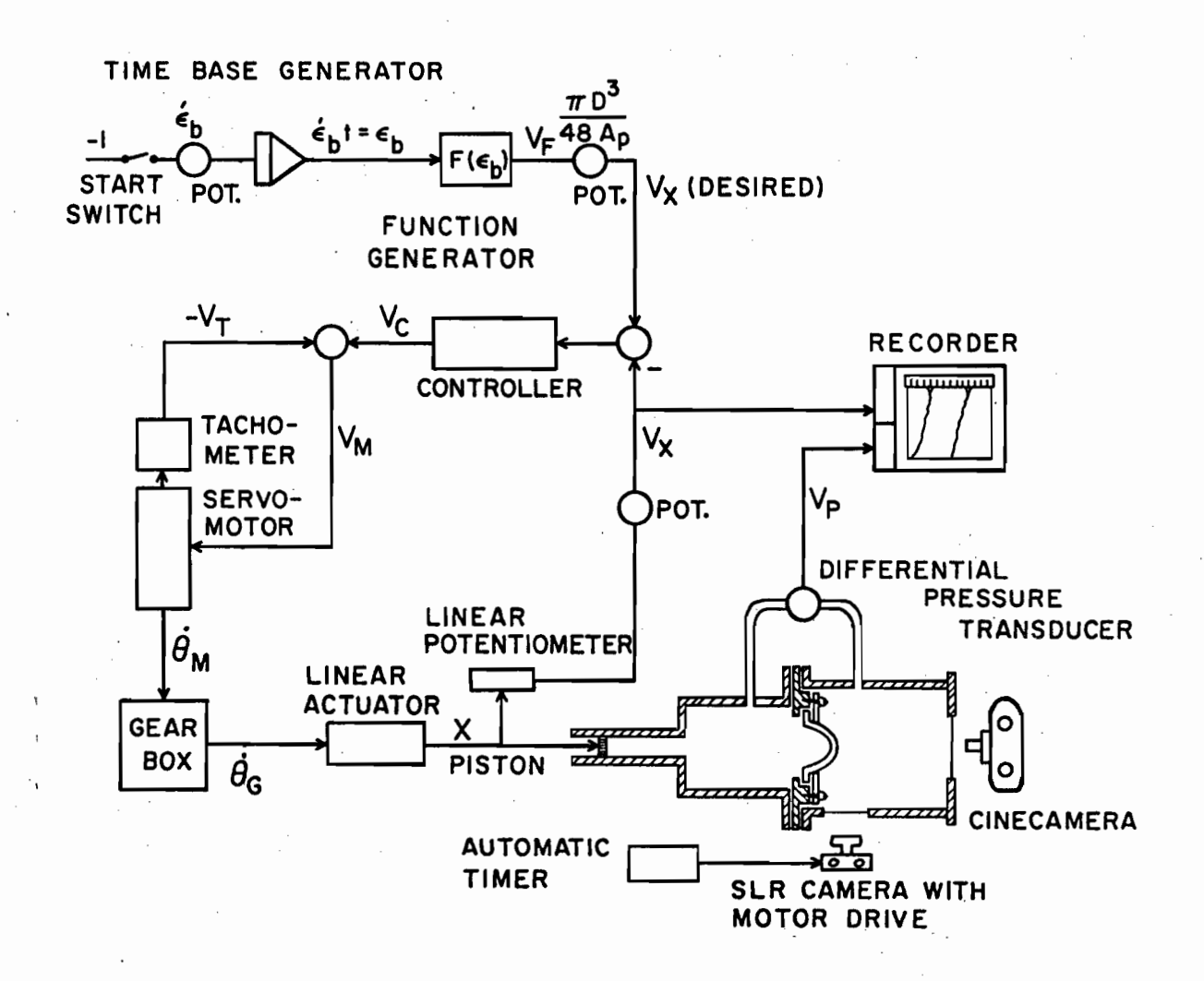


Fig. 3-2. Second Prototype

The second prototype is composed of the following five major components:

#### A. The Mobile Chamber:

This is made of a section of stainless steel (type 304) pipe, 12.7 cm (5") in diameter and 17.8 cm (7") long. Two windows are opened on the sides of the chamber with axes perpendicular to each other and inclined at 45° to the horizon. One end of the cylinder is sealed with a piece of circular glass, 0.95 cm (3/8 in) in thickness and 12.25 cm (4 15/16 in) in diameter, which serves as the third window. There are four tube fittings: a vent on the top for equalizing the inside pressue with atmospheric pressure, a valve on the side for balancing the initial pressure difference between the two chambers, an opening for monitoring the pressure and another valve at the bottom for loading and draining silicone oil.

The heating system consists of an immersion heater (400 W), a thermocouple (type J) and a temperature controller (Thermoelectric 100).

At the other end of the cylinder, a Viton O-ring is positioned to assure proper sealing between the chamber and the clamping ring. The chamber is supported by two arms with bushings which ride on two shaft rods, so that the chamber can move backward and forward to load and unload the

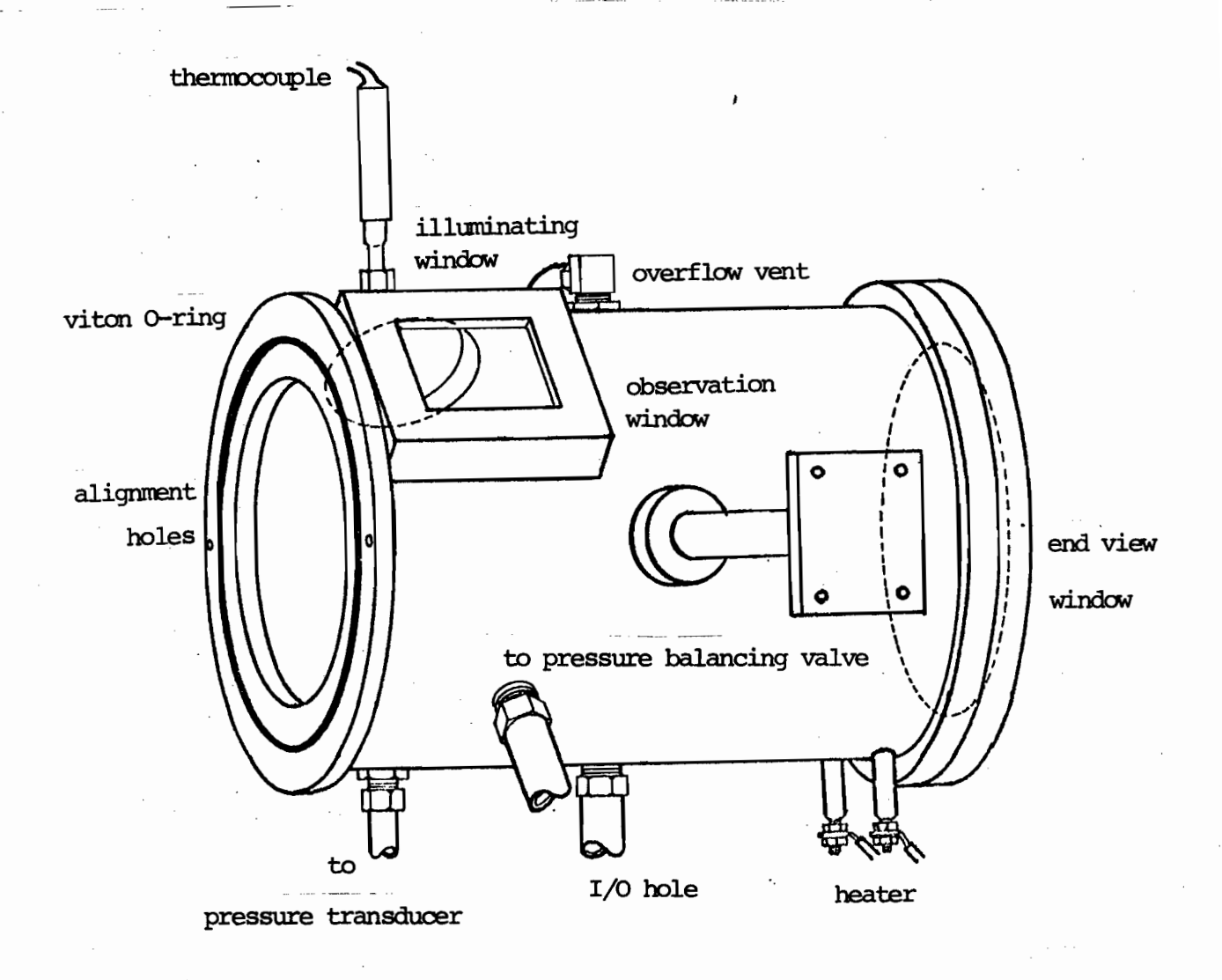


Fig. 3-3. The Mobile Chamber

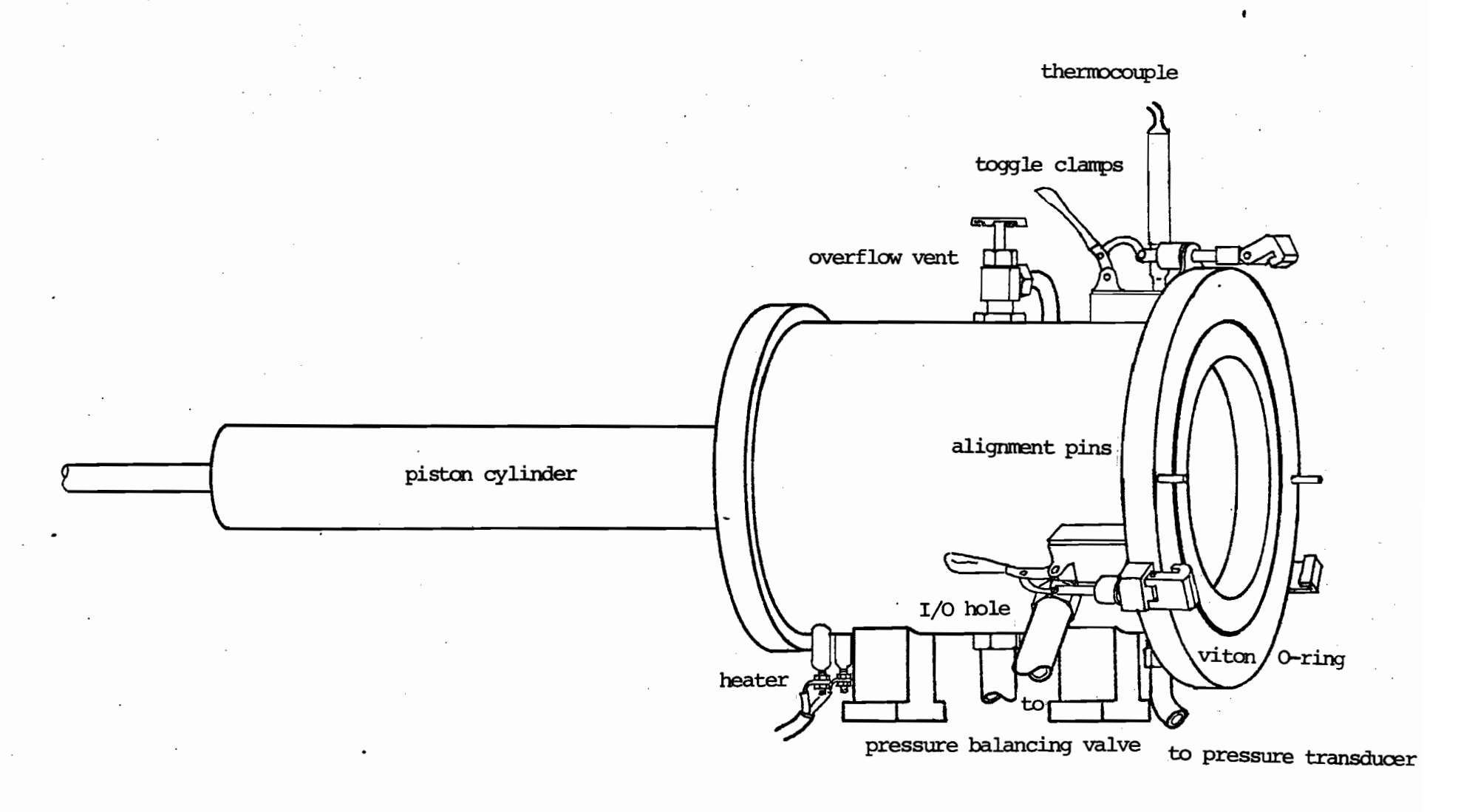


Fig. 3-4. The Fixed Chamber

clamping ring.

#### B. The Fixed Chamber:

This chamber is also made of a section of stainless steel pipe with a 10.16 cm (4") nominal diameter and a 15.24 cm (6") length. Tube fittings are the same as in the mobile chamber.

A plate ring with a Viton O-ring mounted in it is fixed at one end of the chamber. For holding these two chambers and the clamping ring together, three uniformly distributed toggle clamps are installed on the cylinder wall near this end. Two pins are fitted on the plate ring for the alignment of these three parts.

A smaller cylinder with a 2.8575 cm (1 1/8 in) bore is attached to the other end of the chamber. A piston with a 17.78 cm (7") stroke is fitted in the smaller cylinder. This piston is driven by a linear actuator which transforms the rotary motion of a motor shaft into linear displacement.

#### C. The Clamping Ring:

This clamping ring consists of three parts. The main body is an aluminum block, 12.7 cm (5") in diameter, 2.54 cm (1") thick, with a hole 6.35 cm (2.5") in diameter in its center and a groove, 7.62 cm (3") in diameter and 0.3175 cm

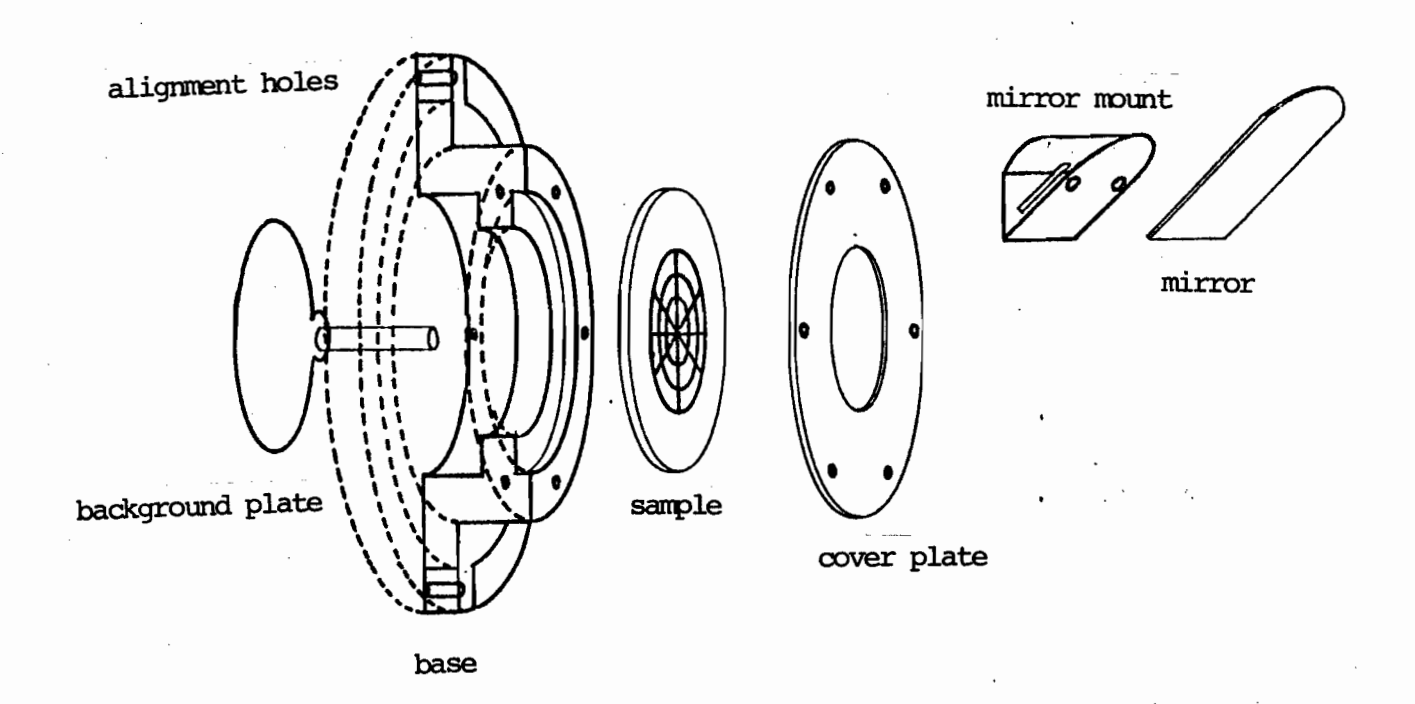


Fig. 3-5. The Clamping Ring

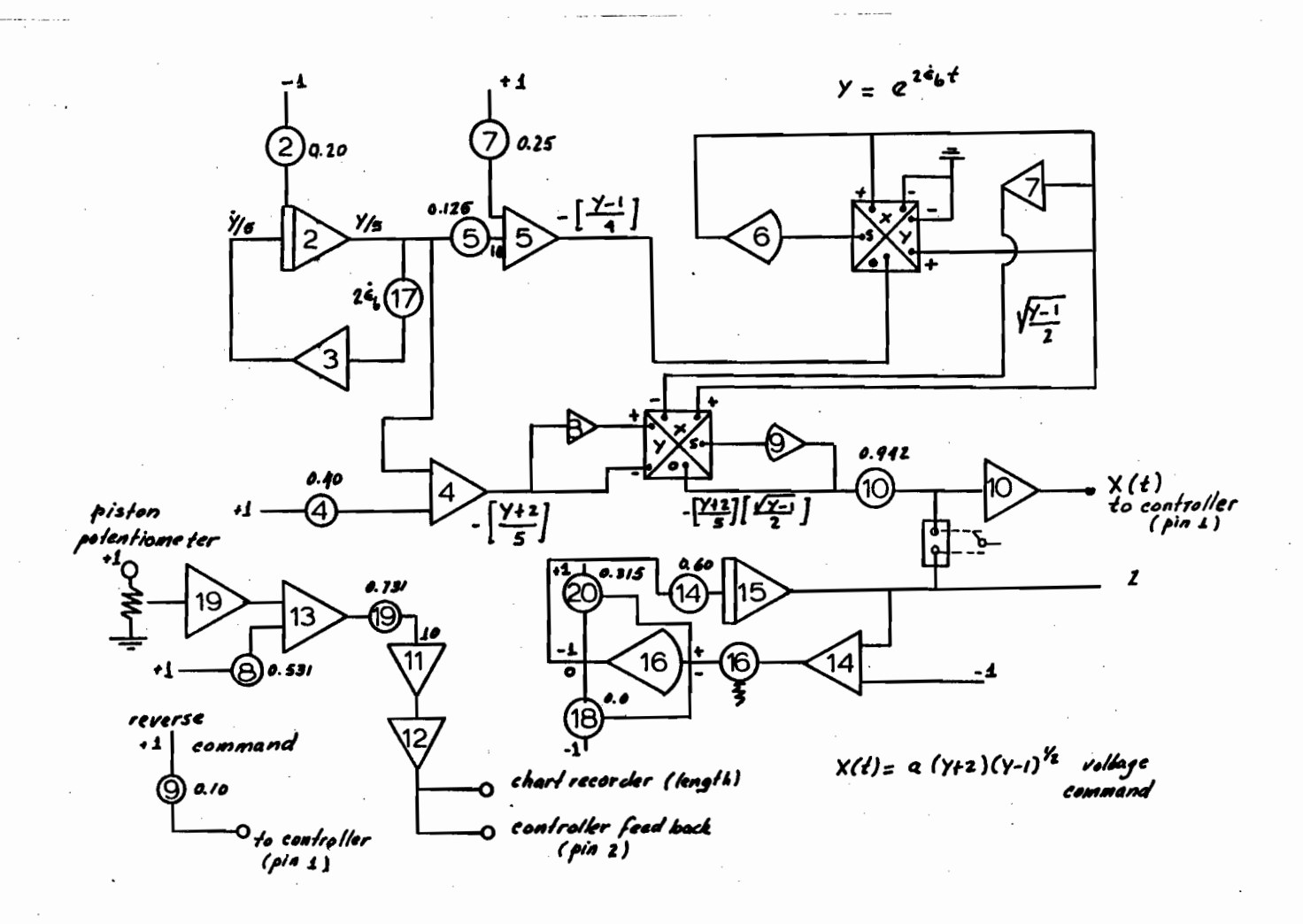


Fig. 3-6. Analog Computer Control System

(1/8 in) in depth to fit the sample disk. An aluminum plate, 12.7 cm (5") in diameter and 0.16 cm (1/16 in) thick with a hole 4.48 cm in diameter holds the sample in place. Six screws are used to hold these two parts together. A smaller white aluminum plate is mounted on the opposite side of the main plate to provide a uniform, opaque background for observation.

#### D. The Control System:

Since strain is governed by the displacement of the piston, which is in turn driven by the motor, the only way to control the strain is to control the rotation of the motor. A d.c. voltage signal following an ideal model is generated by an analog computer (EAI TR-20), and transmitted to the servoamplifier (Jordan AD-7500) which is driving the rotation of the motor (EC-1200). The motor shaft and a gear box of gear ratio 50:1 is connected by a clutch activated by 24 V d.c. The revolving motion is then transformed to the linear displacement of the piston by a linear actuator (pitch = .75 cm/rev). A potentiometer is attached to the piston shaft to provide the feedback voltage signal proportional to position for the analog computer. The block diagram is shown in Fig.3-6.

#### E. The Recording System:

#### a. Pressure :

The pressure difference between the two chambers is monitored by a transducer (Statham PM 6TC ±2.5psid). The signal is conditioned by a transducer readout (Statham Model UR5) and then recorded by a strip chart recorder (HP model 7100B).

#### b. Photographs:

The course of the sheet inflation is followed by taking pictures. The end view photos were taken by a cinecamera (Bolex, 16mm) while the side view photos were taken by use of a motor drive SLR camera (Nikon 35 mm) triggered by a timer.

## 3-4. The Remaining Problems of the Second Prototype:

Although the later design did improve the problems encountered in the first prototype, a great and essential handicap remained: it was unable to generate a constant strain rate deformation. This flaw was due to the following causes: a mistake in deriving the model equation, the limitations of the control system, and the discrepency of the ideal inflation model with the real behavior.

To derive the inflation model, the shape of the bubble was assumed to be a segment of a sphere, so that,

$$x = 2R \sin\beta \tag{3-2}$$

$$\ell = \frac{\mathbf{x} \cdot \mathbf{\beta}}{\sin \mathbf{\beta}} \tag{3-3}$$

when  $\beta = 0$ ,  $\ell_0 = x_0$ 

and 
$$\varepsilon_{\mathbf{b}} = \ln \frac{\ell}{\ell_0} = \ln \left( \frac{\mathbf{x}}{\mathbf{x}_0} \frac{\beta}{\sin \beta} \right)$$
 (3-4)

when  $\beta \rightarrow 0$ 

$$\varepsilon_{\rm b} = \ln \frac{x}{x_0} \tag{3-4a}$$

Failing to notice the fact that the last equation is valid only for a small area near the pole of the bubble, the earlier model equation was derived by applying this approximate equation over the entire surface area of the inflated bubble, even though it is not always a small value, and the following equation was obtained:

$$x = \frac{\pi D^3}{48A_p} \left\{ \left( e^{2\hat{\epsilon}} b^{\dagger} + 2 \right) \cdot \sqrt{e^{2\hat{\epsilon}} b^{\dagger} - 1} \right\}$$
 (3-5)

Rhi-Sausi used an analog computer to generate this function in his experiments.

The strain vs. time curves actually generated are not straight lines, i.e. the actual strain rate is not constant. Only a small section can be approximated by a straight line, which is insufficient to study biaxial extension behavior.

The correct model equation can be derived as follows:

The volume under the spherical bubble is

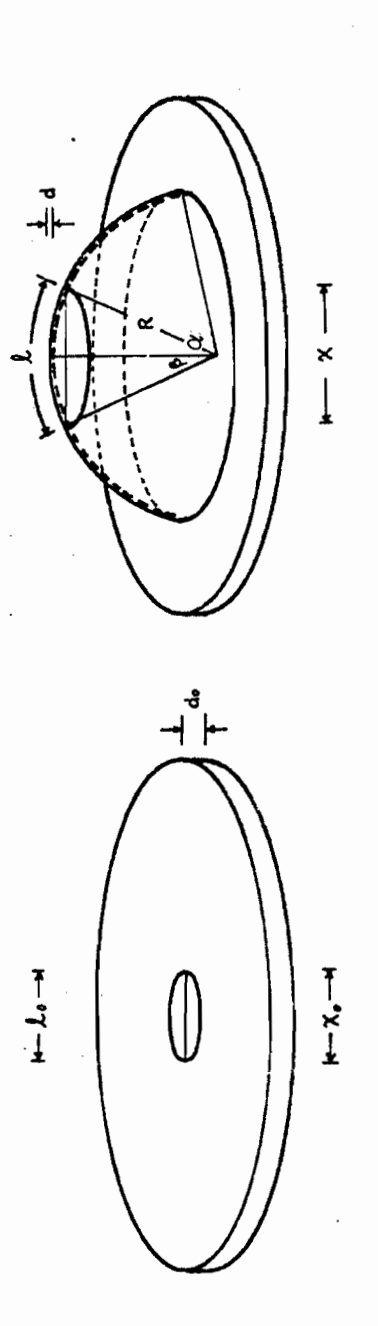


Fig. 3-7. The Sheet Inflation Technique

$$V = \frac{\pi h}{6} (\frac{3}{4} D^2 + h^2)$$
 (3-6)

and

$$D = 2R \sin \alpha$$

$$h = R (1 - \cos \alpha)$$

$$= \frac{D}{2} \tan \frac{\alpha}{2}$$
(3-7)

therefore 
$$V = \frac{\pi D^3}{48} \left( 3 \tan \frac{\alpha}{2} + \tan^3 \frac{\alpha}{2} \right)$$
$$= \frac{\pi D^3}{48} F_1(\alpha) \tag{3-8}$$

The overall stretch ratio is

$$\lambda = \frac{2R\alpha}{D} = \frac{\alpha}{\sin \alpha} \tag{3-9}$$

and since 
$$\varepsilon_b = \ln \lambda = \ln \frac{\alpha}{\sin \alpha}$$
 (3-10)

 $\alpha$  is a function of  $\epsilon_b$ , and,

$$V = \frac{\pi D^3}{48} F(\varepsilon_b)$$
 (3-11)

The displacement function is obtained by dividing V by An, the cross sectional area of the piston,

$$X = KF(\epsilon_b) \qquad K = \frac{\pi D^3}{48A_D} \qquad (3-12)$$

However, this function cannot be generated by an analog computer, and a new control system was then required.

In fact, eq. 3-12 is still an ideal model based on the assumption of spherical geometry, and a constant strain rate is still not obtained. Because the exhensional stress is not uniformly distributed, the inflated bubble does not have a uniform radius of curvature, and this will be discussed in a later chapter.

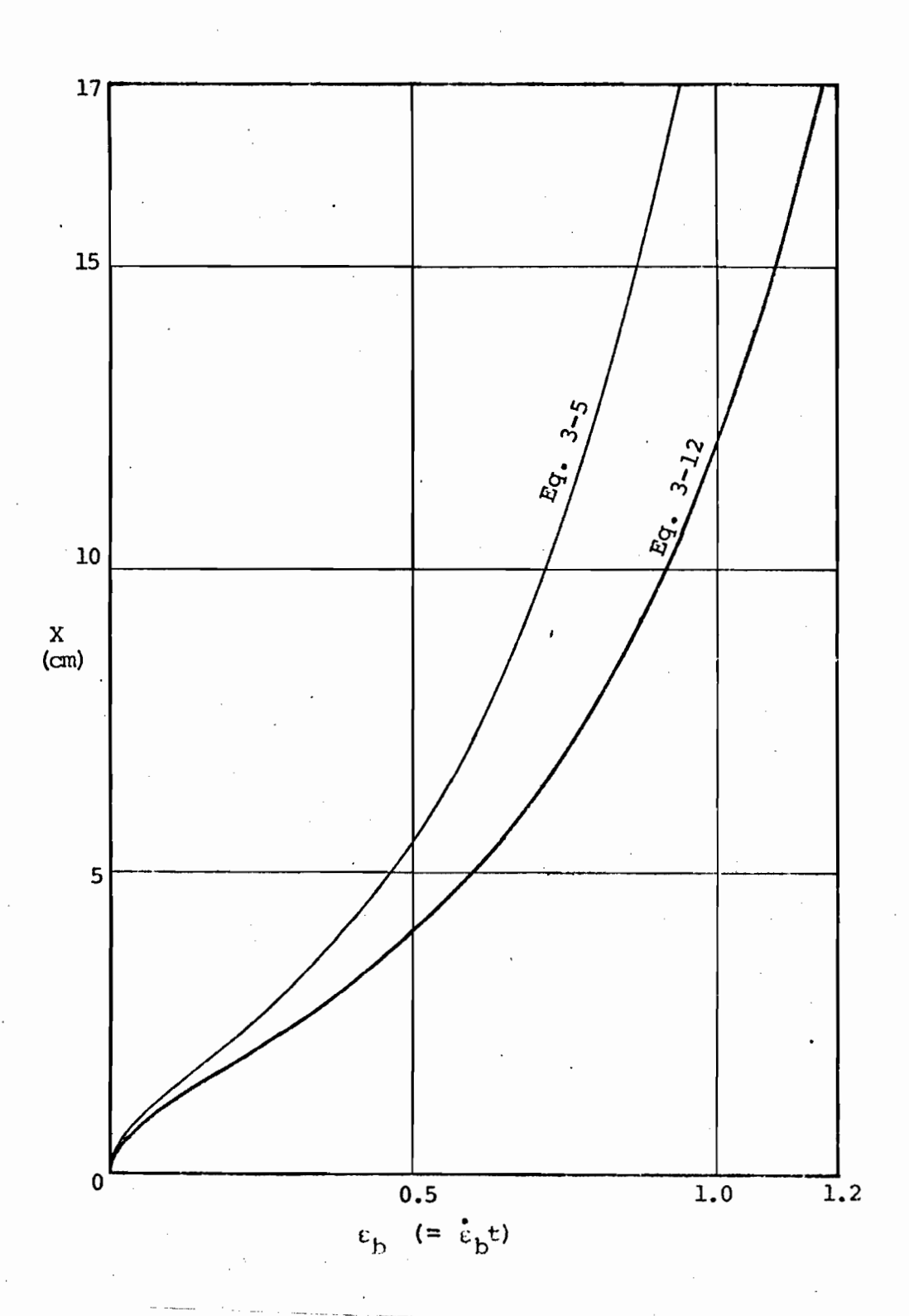


Fig. 3-8. Comparison of Model Equations

#### CH. 4 THE DIGITAL CONTROL SYSTEM

### 4-1. Control Strategies:

### 4-1-1. Analog control versus digital control:

The objective of the control system of the extensioneter is to make the displacement of the shaft follow a model function. There are several ways to accomplish this. The use of an analog computer is attractive, since it is simple to operate, and provides a signal that is continuous in time. Unfortunately, it can not generate the model function given by eg. 3-12.

Unlike an analog computer, the operation of a digital computer is discrete rather than continuous. Also, in order for an analog signal to be processed, it must be converted into digital data, and there is a loss of precision in this step. However, there are also some advantages of a digital control system. First, the digital control system is flexible, because it is a combination of hardware (electronic components) and software (program). As long as it is within the basic ability of the hardware, the modification of the system is accomplished by simply changing the program. This is of great advantage, especially when the model function is to be altered.

Second, experimental data can be stored in the memory of the digital computer. Although an analog signal can be recorded by a recording device such as a chart recorder, still these curves have to be analyzed and converted into numbers. This procedure is a tedious one; on the other hand, the retrieval of digital data from the computer memory can be done immediately after the end of experiment.

Third, with appropriate circuitry, the digital system is much more versatile. The ability of an analog computer is limited to giving an output signal responding to an input electronic signal or time. It is difficult for an analog computer, for example, to turn on or off a switch at an irregular frequency, while it is very simple to do this with a digital system by appropriate programming.

Because of the above advantages, a digital control system was chosen for the improved extensiometer.

# 4-1-2. The selection of digital control type:

Generally there are three types of digital control systems:

## (1) Data-logging Processing and Monitoring:

The digital computer simply reads data from the process and does some data-processing, such as panel

display, log writing, or activating an alarm. Actually, the system is not under the control of the computer. The only benefit is to spare the operator's time on data-logging.

#### (2) Direct Digital Control (DDC):

The role of a conventional controller is played by the digital computer in this type of control system. Process data are converted by an A/D converter into digital signals, and control commands are generated by the computer and sent to the process through a D/A converter. The operation of this type of system is more economical than that of a conventional controller, since a digital computer can handle several processes almost simultaneously.

#### (3) Supervisory Computer control (SCC):

The process is still controlled by conventional controllers, but the set points of these controllers are specified by the digital computer. This type of system is especially suitable for optimal control. The computer calculates the optimum values of set points so that the system can achieve the optimum operation.

Since there is only one process to be controlled in the extensiometer, namely, the displacement of the shaft, both DDC and SCC are suitable. In SCC, a convensional PID controller could be used to drive the servomotor, while the adjustment of the set-point, the desired position of the shaft, could be done by the digital computer through a D/A converter. The accuracy of DDC is less than SCC, because of the limited resolution and discontinuous control. However, experimental results indicate that the maximum error is around 1% for an 8 bit system, and this is considered acceptable. From the point of view of economics, DDC is better than SCC, since a conventional controller is spared. Hence DDC was adopted in the design of the control system for the extensiometer.

# 4-1-3. The selection of the controller function :

Æ

The variable to be controlled is the displacement of the shaft, X, which is the integral of the shaft velocity,  $\mathbf{v}$ , with respect to time. The actual variable to be controlled, however, is the rotational speed of the servomotor,  $\omega$ , which is proportional to the command signal,  $\mathbf{e}$ , a d.c. voltage. The proportional factor is the gain of the servoamplifier,  $\mathbf{K}_{\mathbf{M}}$ . The rotation of the motor is converted into the linear motion of the shaft by a linear actuator; i.e.,  $\mathbf{v}$  is actually proportional to  $\omega$ , and the proportionality is the gear ratio of the gear box,  $\mathbf{K}_{\mathbf{G}}$ , times the pitch of the linear actuator,  $\mathbf{K}_{\mathbf{A}}$ . Thus, these variables can be related to each other as follows:

$$\omega = K_{M} e$$

$$v = K_{A} K_{C} \omega$$

$$= K_{A}K_{G}K_{M} e$$

$$= A \cdot e$$
(4-2)

$$X = \int_0^t v dt = A \int_0^t e dt$$

$$A = K_h K_c K_M$$
(4-3)

where

It is obvious from eq. 4-3 that e is the key in making X follow the model function. There are several ways to generate a suitable e value by use of a digital control system.

#### (1) By imitating a conventional controller:

In a conventional feedback control system, as shown in Fig. 4-1, we have :

$$e = G(X_S - X)$$
 (4-4)

where G is the transfer function of the controller.

However, two problems are encountered when this method is adopted in the control system of the extensioneter. The first is the response lag time that arises from the computational time. The simplest controller function is proportional control, but it is also the most inaccurate; on the other hand, a PID controller is more accurate, but it takes time to compute the response, and this may cause a serious time lag.

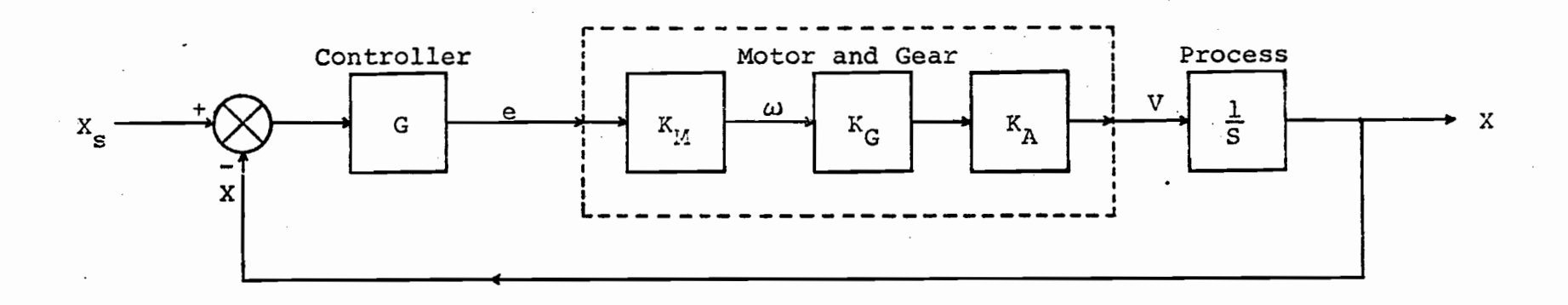


Fig. 4-1. Block Diagram of Conventional Control System

The second problem is the difficulty in obtaining a precise response. Because the position of the shaft, X, is fed to the computer through an A/D converter, whose resolution is only 1/256 of full scale, i.e. for a maximum travel distance of 16 cm, it is 0.0625 cm, the computer can not percieve any change less than 0.0625 cm. Therefore, when X is small, the relative error is quite large, and the computed response is inaccurate, which may make the system uncontrollable. In fact this method is suitable only for an SCC system, since the above two problems do not arise in this case.

#### (2) By using a digital controller function:

There are several popular digital controller functions that have been used for years. However, as in the first scheme, the limited resolution of the A/D converter is still the major cause of the ineffectiveness of the control system. Because the job of the control system is basically a servo type, i.e., set-point adjustment, to avoid serious distortion of the response to the model function, the set-point change must be as small as possible. The step size used is usually 1/256, the same as the resolution of A/D converter. This means that the set-point change is of the same order as the uncertainty in the feedback signal (the limit of resolution), and this will lead to the generation of an incorrect response, i.e. a deviation of the actual displacement from the model.

#### (3) Linear approximation scheme :

The principle of this approach is to represent the model curve by segments of straight lines. Since the slope of a line segment is the velocity of the shaft displacement in that time interval, and the velocity is proportional to the output of the computer, as indicated by eq.4-2, the controlling function consists of the sequence of these slopes for each time interval. The smaller the interval, the closer is the actual response curve to the model. There are two methods to determine the appropriate controlling function:

#### a. By using the average velocity:

The function value for each interval is the slope of the straight line that passes through the two end points, i.e.,

$$D(t) = \frac{X_{s1} - X_{s2}}{t_1 - t_2} \qquad t_1 \le t \le t_2 \qquad (4-5)$$

#### b. By taking the derivative of the model equation :

The function value is the first derivative of the model function at the present position, i.e.,

$$D(X) = \frac{dX_s}{dt} \Big|_{X_s = X}$$
 (4-6)

Eq.4-5 is dependent on time only, while eq.4-6 is dependent on the position. Though theoretically these two controller functions should yield the same response, for the ease of programming, the first controller function is chosen, since it does not have to compute the derivative of the model function. Because of the nonlinear charateristics of the D/A converter output, another term, which is proportional to the difference between the setpoint and the current reading, is added to eliminate this nonlinearity; thus this deviation can be reduced to 0.4% of full scale.

## 4-1-4. Summary:

A direct digital controller was chosen for the control system. The block diagram of this system is shown in Fig. 4-2.

#### Where,

- θ(s) = the Laplace transformation of the control variables
- $\theta(z)$  = the z-transformation of  $\theta(s)$
- $\theta_{D}(z)$  = the z-transformation of the set-point change
- $H_0(s) =$ the Laplace transformation of a zero-order data holder function,  $\frac{1-e^{-Ts}}{s}$
- G<sub>p</sub>(s) = the Laplace transformation of the process functions, an integral, 1/s
- D(z) = the z-transformation of the digital controller function

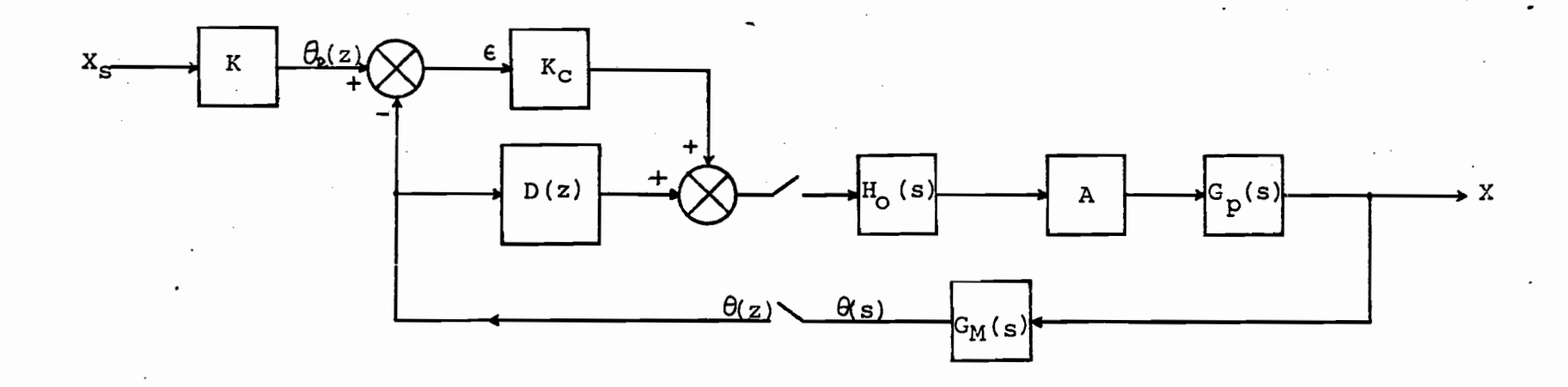


Fig. 4-2. Block Diagram of Digital Control System

K = the proportional gain of the controller

 $G_{M}(s)$  = the Laplace transformation of the measurement function

K = the proportionality that converts the value
 of Xs into an integer between 0 and 255

 $A = K_G K_A K_M$ 

### 4-2. Hardware Description:

The control system is composed of a digital computer, an interface circuit, and the servomotor system that was described in the previous chapter.

### 4-2-1. The digital computer:

The main body of the control system is a Commodore PET minicomputer which is based on an MCS 6502 microprocessor. The PET has a memory capacity of 16 k byte, and the operating language is BASIC, although an instruction SYS enables programming in the machine code. there are also a CRT screen and a tape cassette unit connected to the PET.

### 4-2-2. The interface circuit:

Because the computer does not have integral A/D or D/A conversion ability, it is imposible to drive the servomotor

directly, and an additional interface is thus required.

The most important parts of this circuit are the A/D and D/A converters. The A/D converter (Analog Devices, AD570JD) can convert an analog voltage signal into an 8-bit digital signal in 25 us. When the mode control B&C (Blank and not Convert, pin 11) is brought low, the conversion is initiated. The conversion method used is called successive approximations, which is comparing the input analog signal with the output of an internal D/A converter succesively from MSB (Most Significant Bit) to LSB (Least Significant bit), and the results of comparison are stored in an SAR (Successive Approximation Register). When the conversion is completed, the status DR (not Data Ready) is brought low, which means that the binary number shown on the digital outputs (pin 9 to pin 2) are valid data. When B&C is held high, this IC is in an idle state, and all the 8 output pins as well as  $\overline{DR}$  are at a high level.

Although the AD570 can handle bipolar conversion (+5Vto-5V), in the case of the shaft position reading, unipolar conversion (0to+10V) is used, and the bipolar control (pin 15) is shorted to the analog common (pin 14). Since the reading from the pressure transducer is also to be taken, a multiplexer (Analog Devices, AD7503) is employed for the selection of the input analog signal. To adjust the full scale to 10 V, a  $200\Omega$  trimmer is inserted between the multiplexer output (pin 12) and the A/D converter analog

input (pin 13). Because both the full scale voltage of these two analog signals are not 10 V, they must be conditioned. The pressure transducer output is first conditioned by a conditioner (Analog Devices, 2B31J) then amplified by an operational amplifier (741) so that the digital reading is the pressure value in units of 10Pa. The position reading, the output of a potentiometer, is connected to a voltage follower ( $\mu$ A310HC) to avoid the loading effect, and then amplified by another 741. A 2.5 V voltage reference and a  $2k\Omega$  trimmer are used to adjust the zero point of the position reading.

The data acquisition process is operated through a PIA (Peripheral Interface Adapter, Motorola, MC6821), which is accessed through 4 addresses in the PET's memory, 28672 to 28675 by using CMOS gates (4001, 4002, 4012, 4069) as the address decoder. There are two data ports on each PIA, called sides A and B. Each port is composed by an 8-bit direction-programmable data bus and 2 interrupt /peripheral To activate this IC chip, the two control control lines. registers, CRA (at 28673) and CRB (28675) are brought to 0 so that the bit directions of each data bus can be programmed. By assigning a value 1, the data line is able to send out a signal, while a value 0 enables this line to receive a signal. In this interface circuit, bus A is used to receive the data from the A/D converter, so a number 0 is assigned to the address 23672, which is the location of the DDRA (Data Direction Register A); while for port B, a number F8<sub>H</sub> (248) is assigned to DDRB (28674), so that, in bus B, bit 7 is used to activate the conversion and enable the multiplexer, by connecting to B&C and EN (pin 3 of AD7503), bits 4-6 are used for channel selection of the multiplexer, bit 3 is used to trigger the camera, bit 2 is for sensing DR, and bits 0 and 1 are connected to pins 18 and 1 of AD570 to provide two extra bits of the converted data, but their accuracy is not guaranteed. Then a number  $34_{\rm H}$  (52) is and CRB to enable the data assigned to both CRA transmission. By bringing low bits 4 to 7 of bus B, channel 1 of the multiplexer is chosen, and the digital number on bus A is the position reading; while if bit 4 is brought high while keeping the other two bits low, the pressure reading on channel 2 is chosen and appears on bus A. The camera is triggered when bit 3 is held low and deactivated by holding high the bit.

Because the analog signal change during the A/D conversion period is much smaller than 1 LSB (0.4% of full scale), a sample and hold amplifier is not necessary in this interface circuit.

The D/A conversion is performed by the other part of the interface. The digital signal corresponding to the shaft moving speed is transmitted to a D/A converter (Analog Devices, AD558JD). There are two control inputs,  $\overline{CS}$  (not Chip Select, pin 10) and  $\overline{CE}$  (not Chip Enable, pin 9).  $\overline{CE}$  is connected to BR/ $\overline{W}$  (Buffered Read and not Write) of the PET,

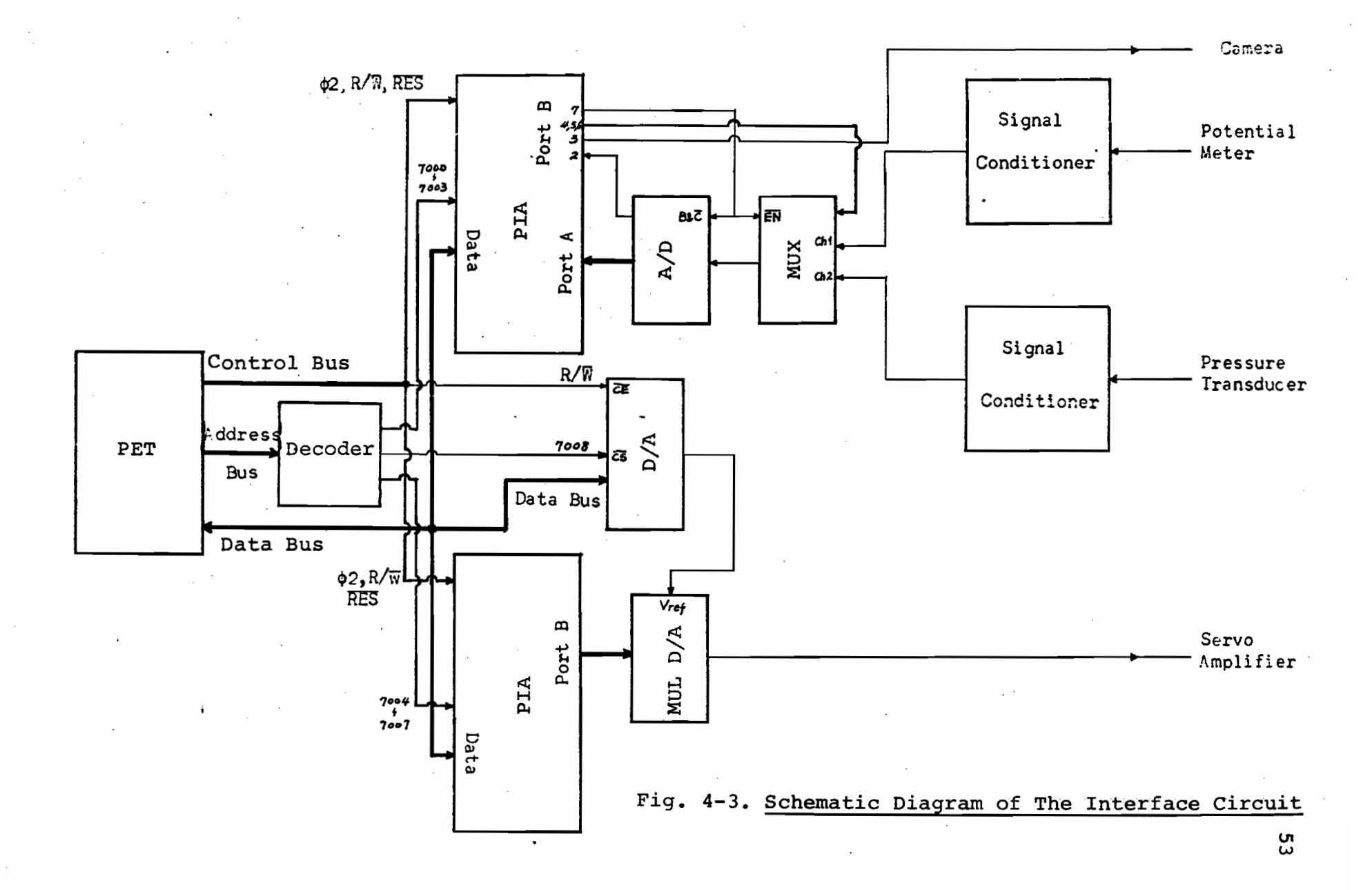
and  $\overline{\text{CS}}$  is connected to the output of the address decoder, which is made up of several CMOS logic gates, and gives the D/A converter the address 28680. The analog output level is adjusted to 0 to 2.56 V by connecting pin 14 to pin 15. To enable the computer to control the output range, the analog output of AD558 (pin 16) is connected to a multiplying D/A converter (Analog Devices, AD7523), by which the signal is multiplied by a number from -127/128 to +1 so that the maximum 8-bit digital number, 255, corresponds to the maximum rotational speed of the motor. Like the A/D converter, this multiplying D/A converter is under the control of a PIA, and thus is located at 28678. number 128 is assigned to this chip, the analog output is 0 V, for any number greater than 128, the output is positive, whereas for numbers smaller than 128, the output is negative, hence the motor can rotate bidirectionally.

Fig. 4-3 shows the schematic diagram of this control system.

## 4-3. Description of the Software:

Two programs are used to control the rotation of the motor, since there are two stages in the experimental procedure.

### 4-3-1. The program "TEST":



The object of this program is to obtain the empirical relationship between the position, X, and the strain of the sample,  $\varepsilon_{\rm b}$ . The block digram is shown in Fig. 4-4 (a).

In the first section, the direction of the data ports of the two PIAs in the interface circuit are programmed by POKing numbers to their addresses. Because all 8 bits of port A at address 28672 are used for reading data from the A/D converter, the number 0 is POKEd to that address. Because bit 3 to bit 7 of port B at address 28674 are for controlling the multiplexer and the camera, and bits 0 to 2 are for receving messages from the A/D converter, the number 248 is POKEd to 28674. Since all the 8 bits of the other port B at 28678 are for sending data to the multiplying D/A converter, the number 255 is POKEd to 28678. Afterward, the number 52 is POKEd to each control register: 28673, 28675, 28677, 28679 to turn the corresponding ports into data I/O ports. Then 136 is POKEd to 28674 to hold the action of A/D conversion and camera. To halt the motor, 128 and 0 are POKEd to 28678 and 28680 respectively. At this moment, the system is ready to drive the motor and hence the movement of the piston.

Because the experiment is to be carried out so that the piston speed is constant, the operating parameter, V, is specified in the second section of the program. In addition to this, the value of A, the factor for converting a digital signal to actual velocity, as well as the proportional

controller gain, B, is also specified. Thereafter, the schedule of the experiment is determined. First, the total time required, TT = 17/V\*60, in the units of 1/60 second, is calculated. Next, the time interval for photographing is D=TT/30, since there are 31 pictures to be taken. And finally, the time interval for changing the set point is T=TT/255. Then the velocity is converted into a digit number, and the forward multiplier, 90, is POKEd to 28678. The system is now ready to start the experiment.

The experiment is now carried out in the third section. The piston is to move at a constant velocity, and to achieve this, the postion signal is received and compared with the set point; the output of the computer is then calibrated proportional to the error. The camera is taking pictures periodically. The first step of this section is to take the initial picture of the sample; then the clock is set to zero. After that, the position signal is read and the digitized velocity is calculated and converted into a voltage signal, which drives the motor. Then the clock is checked for photographing and for changing the set point. When the clock reaches the total required time, TT, the numbers 0 and 128 are sent to the addresses 28680 and 28678 respectively to stop the motor. The experiment is thus completed at this moment.

In the last section, the piston is moved back to the initial position, which is done by POKing 255 to 28678 and

50 to 28680. An optional part of this section is for printing out the position readings against the set points to check if the piston is following the desired curve, a straight line. Usually the difference is within 0.4% of the full scale.

By analyzing the results obtained from the first program, an empirical curve of X against  $\epsilon_b$  can be obtained and thence used in the second program.

### 4-3-2. The program "TST1":

The actual experimental procedure is executed by this program, of which the block diagram is shown in Fig. 4-4 (b)

The basic structure is almost the same as "TEST", except that since the piston velocity is not a constant, the set-point values must be loaded into the memory of the PET, and an additional section for reading in these data is included prior to the first section of the program.

Since the pressure reading is needed, the controlling section (third section in TEST) is modified so that when the camera is triggered, the pressure reading is taken simultaneously.

To obtain the values of pressure reading in a

hard-copy form, the last section is also modified to print out these data with a printer.

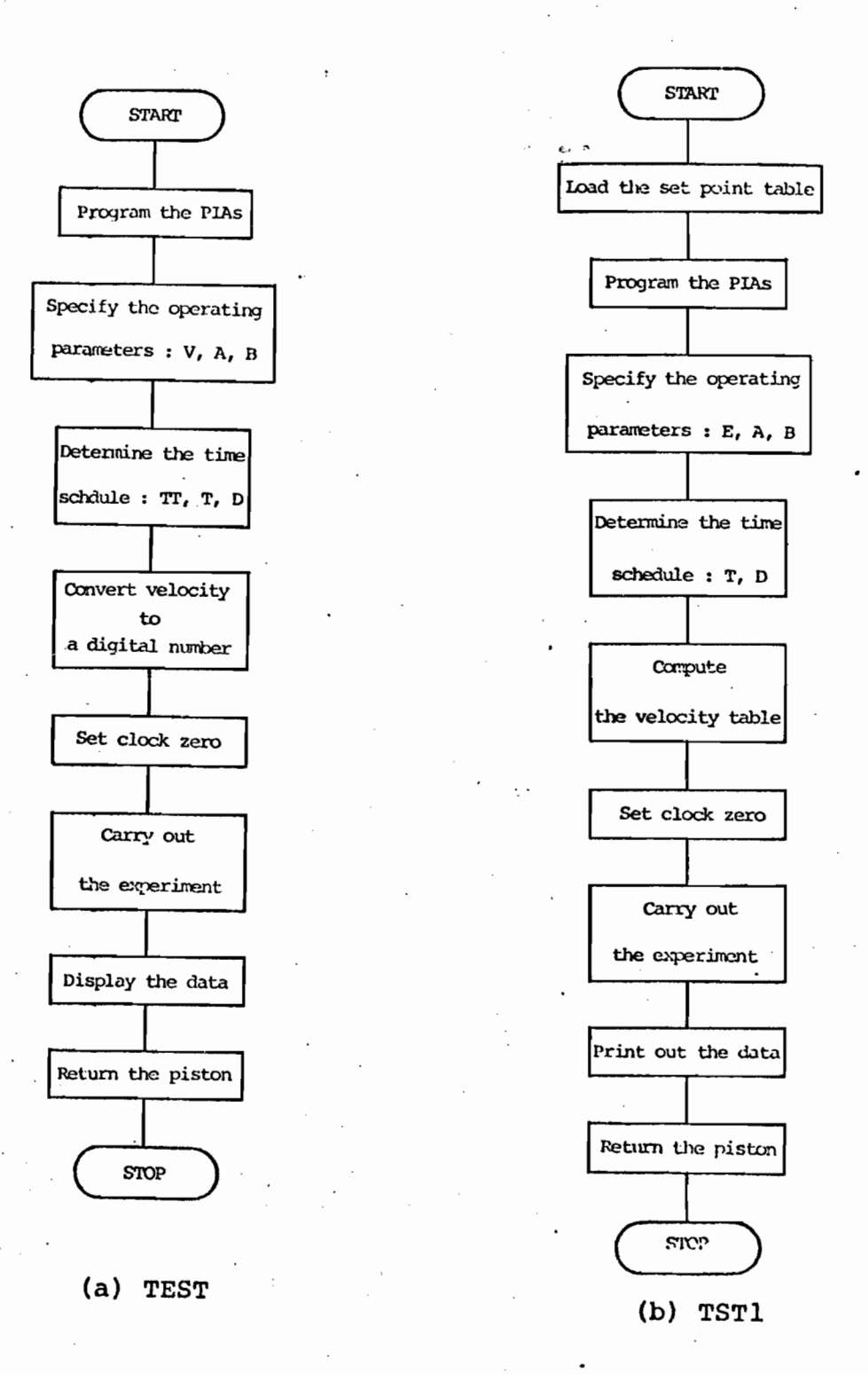


Fig. 4-4: Flow Chart

#### CH. 5 EXPERIMENTAL PROCEDURES

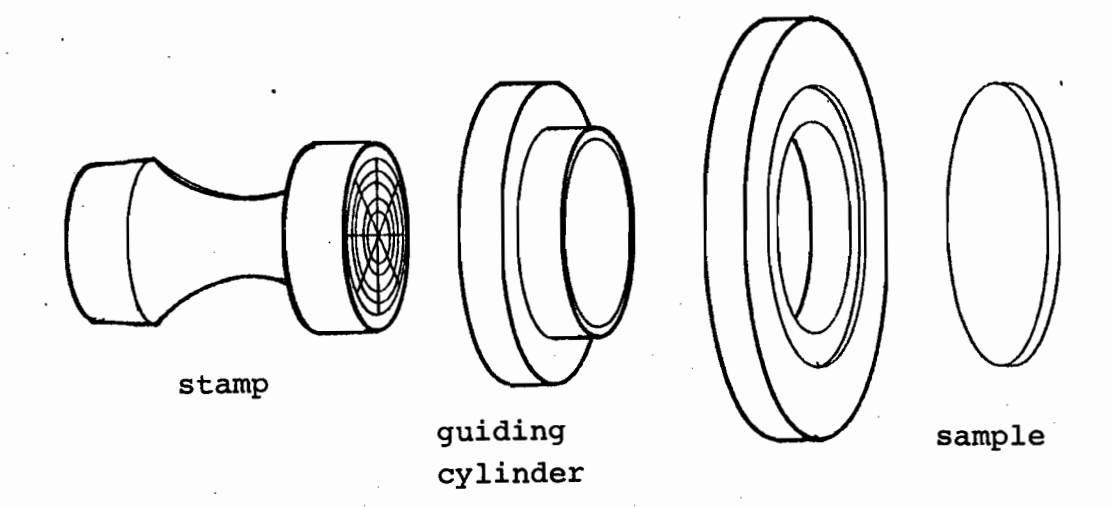
## 5-1. Sample Preparation:

The test samples are prepared by compression molding. The resin particles are loaded into the mold, which is a sandwich of three stainless steel plates. There is a 3" diameter hole in the middle plate, whose dimensions are 6" by 6" by 1/8". To improve the surface smoothness of the sample, two pieces of aluminum foil are inserted between the outer plates and the resin particles. This mold is placed in a hydraulic hot press, maintained at 190°C for 15 minutes and then water-cooled. The variation in the sample disk thickness is found to be less than 0.1%.

To provide the marks for monitoring the strain, a grid is stamped on the sample disk. However, these marks become indistinct at high strain, and one more layer of ink is applied to the center ring of the grid, which is the one of main interest.

The grid stamping kit consists of a ring similar to the clamping ring and a guiding cylinder, to center the rubber stamp, which is mounted on an aluminum cylinder.

#### 5-2. Loading the Instrument:



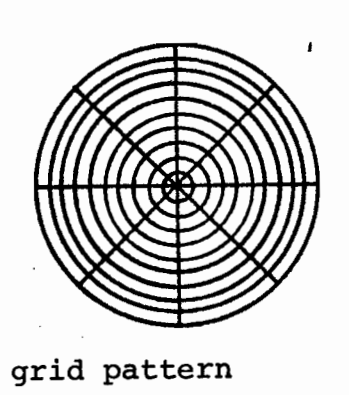


Fig. 5-1. Stamping Kit and Grid Pattern

First, the sample disk is placed on the base of the clamping ring, and then the cover plate and the mirror mount are fastened together with the base by means of screws. The whole clamping ring is next installed between the two chambers by letting the alignment pins pass through the holes on the clamping ring. Finally, the mobile chamber is closed and fixed by the toggle clamps.

The oil (Dow Corning 200 fluid, 50cs) is heated up to about the experimental temperature (130°C for LDPE, 160°C for PS, 170°C for HDPE) and then pumped into the chambers. To prevent air from being trapped in the fixed chamber, the vent on the top is opened until oil flows out. Because the path to the fixed chamber is smaller than that to the mobile chamber, it is suitable to fill the fixed chamber first, then let the oil flow into the mobile chamber. When the oil level reaches a mark on the observation window, the valve is closed and the temperature controllers are switched on.

To eliminate any pressure differential between the chambers prior to inflation, both the loading and draining valves are opened. However, since the rates of temperature rise are different, the vent on the fixed chamber should be opened occasionally to allow the overflow of any extra volume of oil.

## 5-3. Operation of the Extensiometer:

During the experiment, the operations involved are the control of the piston speed, the measuring of the pressure, and the photographing. These three operations are all done automatically by the new control system. The required manual operations are the preparatory steps: switching, program-loading, and program-running. These operations are described below.

# 5-3-1. Switching:

## (1) The elctronic circuit:

There is an order in switching on these circuits: first is the interface, then the PET. This is because when the PET is turned on, it clears all its memory automatically, and since the interface can be regarded as eight memory spaces in the PET, it is also cleared, or reset to the null state, which assures all the components are in proper initial condition.

# (2) The motor sytem:

The servoamplifier can only be turned on after the interface has been initiated; that is, when the PET is asking for operating parameters. This is because when the interface is reset, the output to the servoamplifier is not zero, and this causes the motor to rotate, which is not desired.

After switching on the servoamplifier, the clutch can be turned on if the motor is not rotating. If the motor is rotating, the computer must be checked to see if any problem exists.

#### (3) The motor drive camera:

The switch is turned on at the same time as the motor system for the same reason.

(4) The illuminating lamps and the chart recorder:

They can be turned on any time.

#### (5) The valves:

When the experiment is over, open all the valves to drain the oil.

#### (6) The thermal controller:

Once the oil temperature reaches the set point, when the computer is ready to start the experiment, i.e., when it is asking to type in the charater "A", the controller should be turned off to eliminate optical distortion due to natural convection flow. Because the switching can cause a surge of current, which in certain situations may lead the computer to lose control, it is

recommended to type "A" without pressing "RETURN" before the switching.

# 5-3-2. Program-loading:

Æ

The loading procedure is described in detail in the PET manual. Generally, first type in LOAD "TEST" (or "TST1") and press RETURN, then follow the instructions of the computer. To assure that the program can be found, it is advisable to rewind the tape to the beginning.

# 5-3-3. Program-running:

After the program has been loaded, type in RUN and press RETURN, then follow the instructions of the PET.

There are several stop points that must be noticed. When the computer is asking for operating parameters, it is time to turn on the servoamplifier and the camera. When the computer is saying "READY TO GO, TYPE A", it is time to turn off the heater when the temperature reaches the set point. When the experiment is over, the program is stopped and the computer gives a message saying "BREAK AT 200" (or 340 in TST1). This is the time to decide if the experiment was successful. If it was, type "CONT" to continue the program and type "P" when the computer is asking if a hard copy of data is needed, otherwise, type "R" to move the piston back to the original position to prepare for the next experiment.

## 5-3-4. Unloading the Extensiometer:

When the computer is saying "READY TO RESET, TYPE G", it is the time to check if the chambers are empty. When they are empty, type in the character and press RETURN. Then open the chambers and remove the clamping ring.

If no further experiment is to be carried out, turn off the servo motor and clutch first, then the interface and the computer.

# 5-4. The Adjustment and Calibration of the Control System:

## 5-4-1. The calibration of the pressure transducer:

The transducer is calibrated by applying a hydrostatic head to its two ports. This head is produced by using two burettes filled with silicone oil. The pressure difference is equal to the difference of the two liquid levels multiplied by the density of the oil. The output 2 of the signal conditioner 2B31 is then adjusted by tuning trimmer#1 so that the converted digital signal is equal to the value in units of 10Pa. The setup is illustrated in Fig. 5-2.

Because the operational amplifier has an offset voltage, which will cause error in the output, trimmer#2 is tuned to eliminate this offset. When the input voltage is

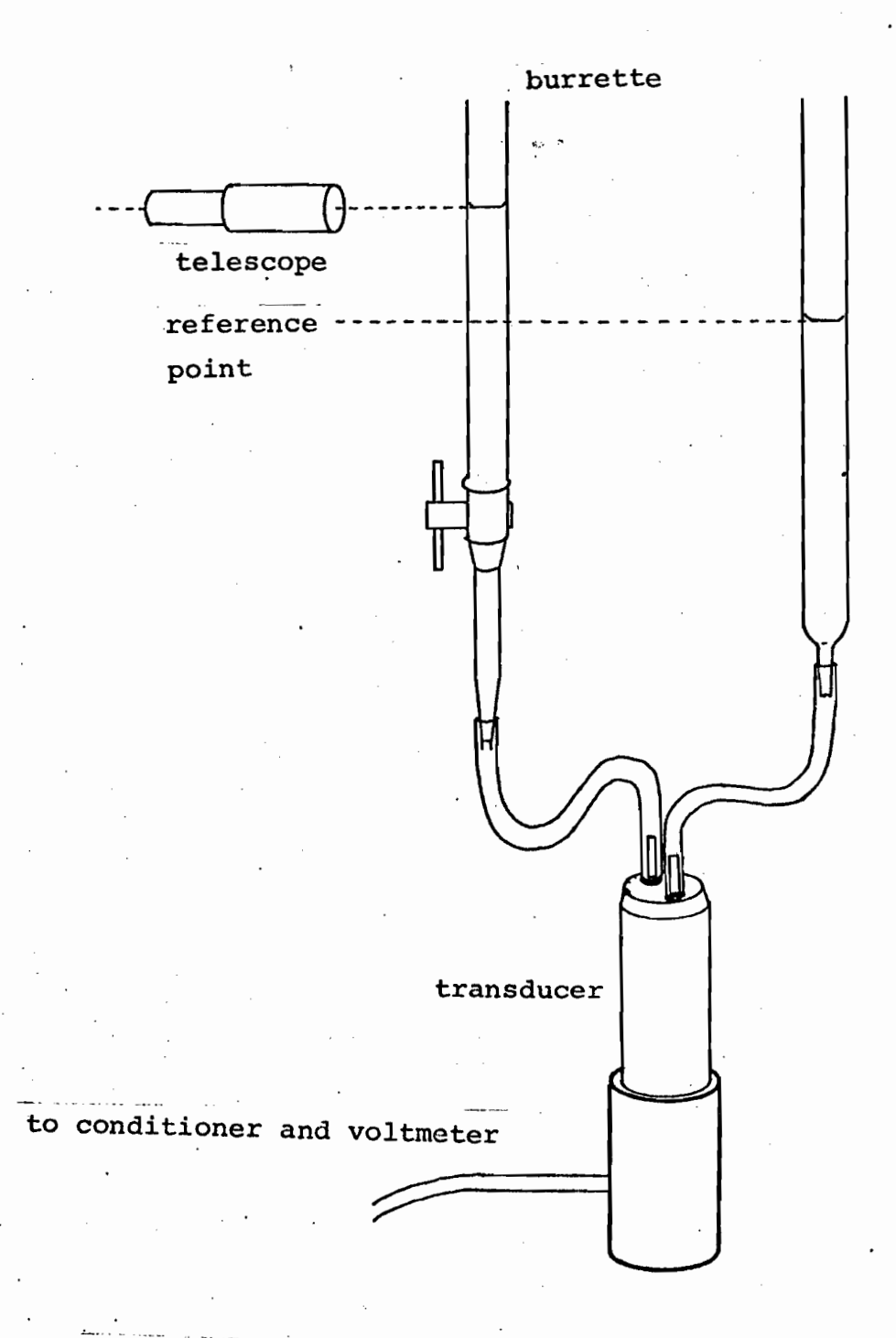


Fig. 5-2. Setup for calibrating Pressure Transducer

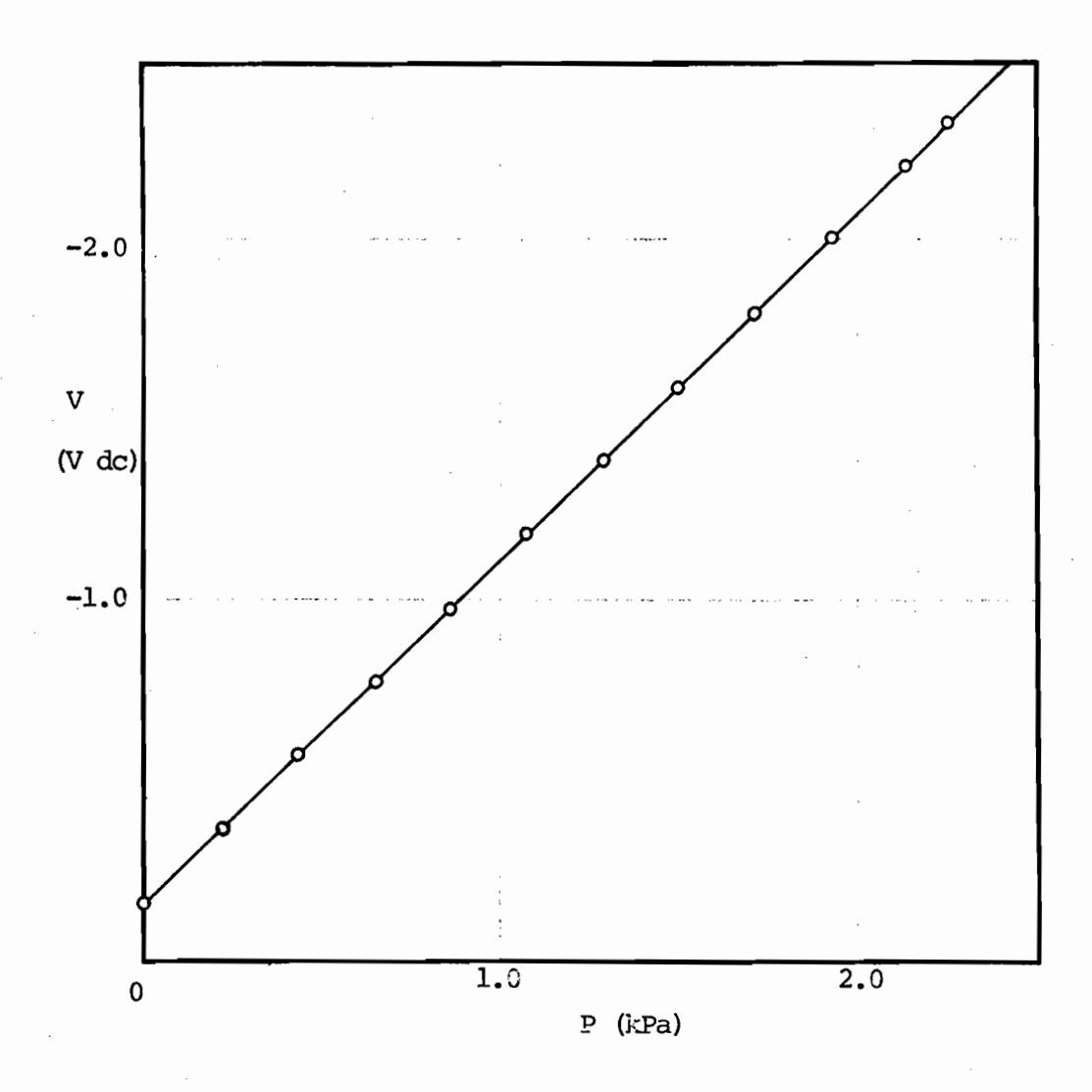


Fig. 5-3. Pressure Transducer Calibration Curve

zero, the output (TP2) should be adjusted to 0 V dc. Then trimmer#1 is adjusted to a suitable position. When the liquid levels are the same, trimmer#3 is tuned so that the output is 0 V dc.

## 5-4-2. The zeroing of the position reading:

After shorting the position reading inputs, the output of the voltage follower (TP4) is nullified by tuning trimmer#5; then TP5 is nullified by bringing TP3 to zero by tuning trimmer#4 and adjusting trimmer#6. Afterward, by POKing 8 to 28674, the voltage at TP7 should be less than 0.03 V dc when the piston is at its zero position, and equal to 9.862 V dc when the piston is at its maximum position. This requirement is achieved by tuning first trimmer#7 to bring TP7 close to 10 V dc and then returning the piston to its zero position. Then tune trimmer#4 to nullify TP7. By repeating this procedure several times, the piston reading is zeroed.

### 5-4-3. The calibration of the D/A output:

The output level of AD558 can be selected to be either 10 or 2.56 V dc by switching the microswitch. For controlling the motor, the latter level is used. As for the multiplying D/A, trimmer#1 and #2 are for offsetting the two operational amplifiers. Because the output of this D/A is very stable, trimmers #3 and #4 need not be adjusted.

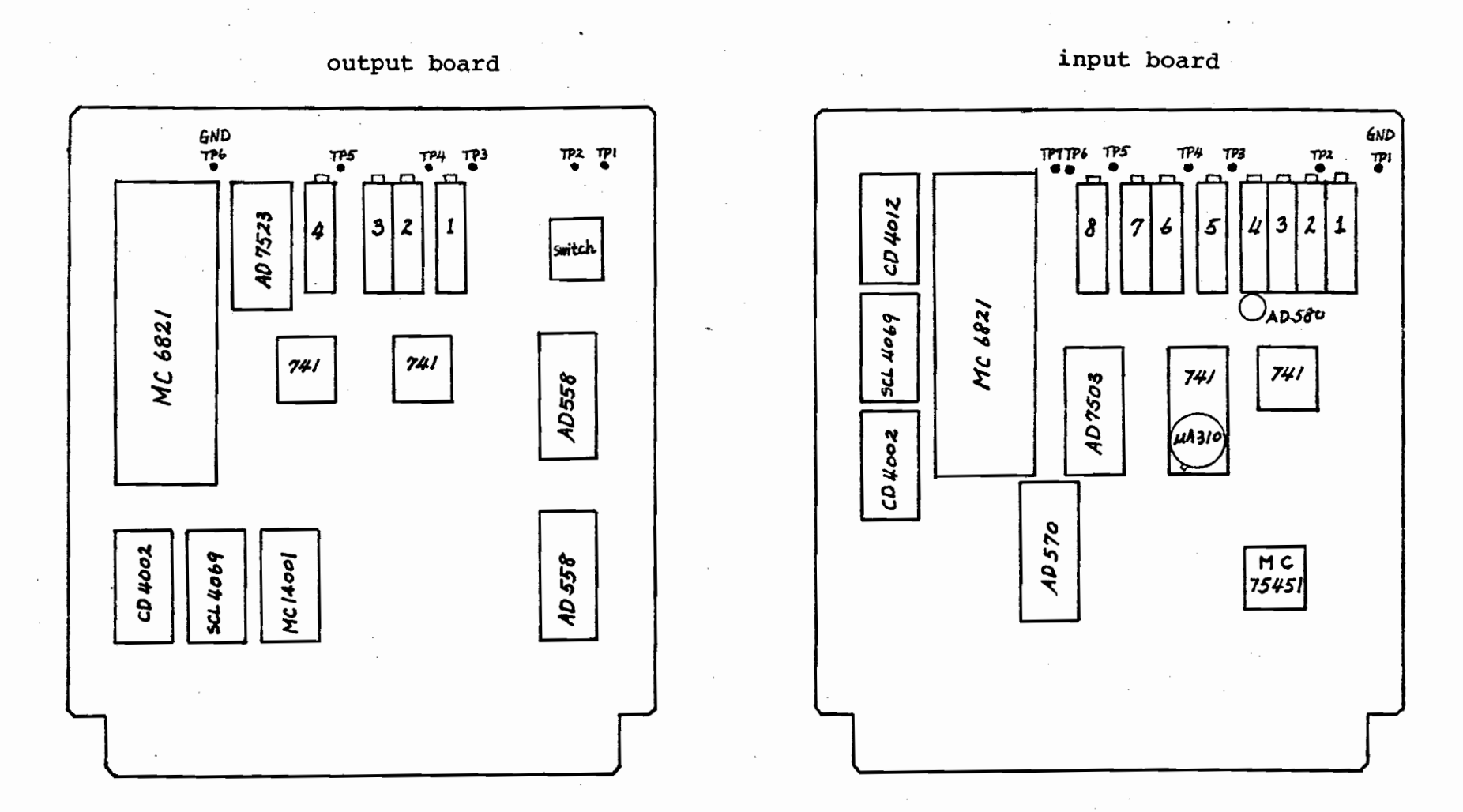
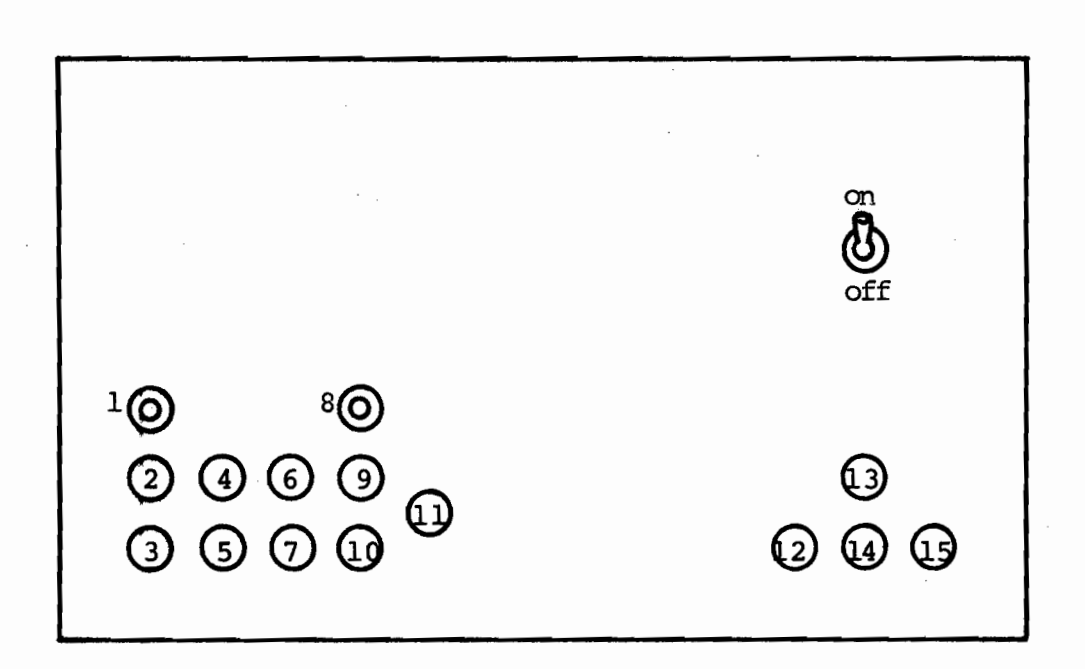


Fig. 5-4. Layout of circuit boards



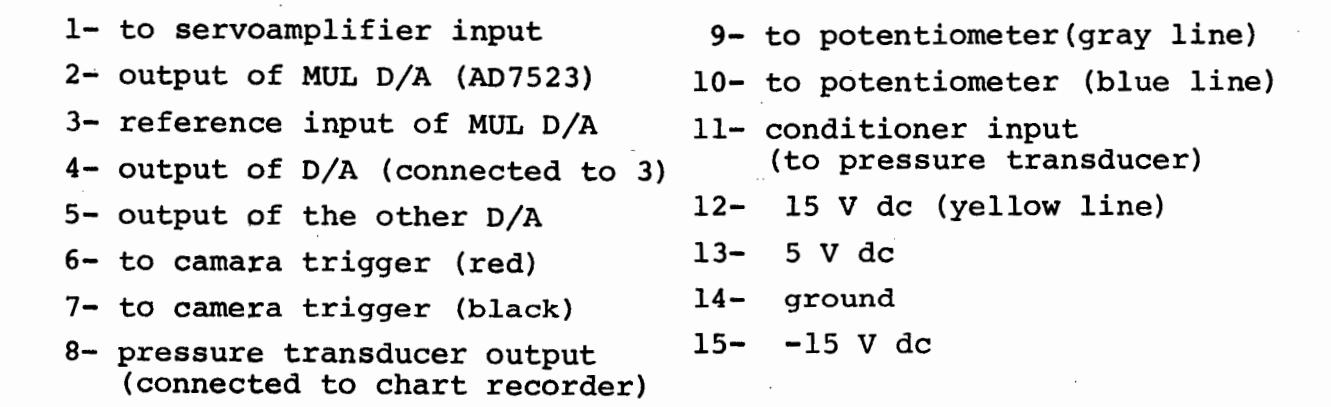


Fig. 5-5. Front view of the interface circuit case

#### Ch. 6 DETERMINATION OF MATERIAL FUNCTION

## 6-1. Data Analysis Procedure:

The objective of this experiment is, first, to obtain a strain vs. time curve to check the constancy of the strain rate; second, to obtain a stress growth function curve; and third, if the stress growth function reaches its steady state value, determine the biaxial extensional viscosity. To calculate these terms, several quantities are required that are obtained by analyzing the photographs taken in the course of the experiments.

The developed negatives are made into slides and are projected on the wall, so that the images are about 15 times actual size. All the measurements are made on the innermost circle of the grid stamped on the sample. Two perpendicular diameters are measured, and the average diameter, x, is calculated.

In determining the radius of curvature, there are several problems that contribute to uncertainity in the value observed.

(a) Because the sample becomes transparent at the experiment temperature, the contrast between the

background and the bubble is very poor, and it is difficult to determine the exact location of the curve.

- (b) The image may be distored due to the natural convection flow in the course of heating. This happens mostly at the beginning of the experiment, and the result is completely unanalyzable.
- (c) Because of the non-uniform temperature distribution, the shape of the bubble gradually deviates from a perfect sphere, and it becomes difficult to determine the exact radius of curvature. This happens mostly near the end of the experiment.

There are two methods for determining the radius of curvature:

(1) The superimposed grid method:

The radius is determined by superimposing a grid of arcs of different radii of curvature on the side view of the bubble, and trying to match one of the arcs to the bubble.

(2) The secant method:

The radius is determined by selecting an appropriate arc on the side view, taking its chord, X,

and its height, h, and using the equation :

$$R = \frac{h}{2} + \frac{x^2}{8h} \tag{6-1}$$

Because in most of the photographs, the side view images are not clear enough, the whole curve, especially the section near the pole, is not obtainable. However, a few segments are still recognizable, and the secant method is more reliable than the superimposed grid method, since one curve can be matched by several arcs of different radii.

## 6-2. The Determination of the Strain:

There are two different measures of the biaxial extensional strain that can be used in the sheet inflation method, these are:

(1) The Longitudinal Strain:

$$\varepsilon_{b} = \ln \frac{\text{Arc AB}}{x_{0}}$$

$$= \ln \left(\frac{x}{x_{0}} \frac{\alpha}{\sin \alpha}\right)$$
(6-2)

(2) The Latitudinal Strain:

$$\varepsilon_{b} = \ln \frac{\pi x}{\pi x_{0}}$$

$$= \ln \frac{x}{x_{0}}$$
(6-3)

When the angle  $\alpha$  is small, these two relationships

give approximately the same value, but as  $\alpha$  becomes larger, the difference grows, Due to the uncertainty in the measurement of the radius of curvature, the first measure will be less accurate, and the second measure is therefore preferred.

## 6-3. The Calculation of the Stress:

The stress can be obtained from a momentum balance on a spherical segment. The tensile force at the edge of this curved shell is given by the tensile stress times the area of this "band" at the edge, i.e.,

$$F_{T} = T\pi x d (1 - \frac{d}{2R})$$

$$\approx T\pi x d \qquad (6-4)$$

Because this body is symmetrical, the r-component resultant is zero, and the z-component is equal to

$$F_{pz} = \frac{\pi x^2}{4} P \tag{6-5}$$

or, 
$$T\pi dx \sin \beta = \frac{\pi x^2}{4} P$$

thus, 
$$T = \frac{Px}{4d \sin \beta}$$
$$= \frac{PR}{2d}$$
 (6-6)

Because the thickness d cannot be measured directly, it must be obtained by taking account of the thermal expansion effect. Thus, for LDPE at  $130^{\circ}$ C, the initial thickness is 0.365 cm, and for PS, 0.348 cm at  $160^{\circ}$ C.

The volume of a sector of a sphere is

$$V_s = \frac{2}{3}\pi R (1 - \cos \beta)$$
 (6-7)

Assume that the thickness in the region near the pole is uniform, so the volume of the shell is,

$$V = \frac{2}{3}\pi \{R^3 - (R - d)^3\} (1 - \cos \beta)$$

$$= \frac{2}{3}\pi (1 - \cos \beta) (3R^2d - 3Rd^2 + d^3)$$

$$= 2\pi R (1 - \cos \beta) \{(\frac{d}{R}) - (\frac{d}{R})^2 + \frac{1}{3}(\frac{d}{R})^3\}$$

$$\approx 2\pi R^2d(1 - \cos \beta)$$
(6-8)

while the oiginal volume is

$$V = \frac{d_0 \pi x_0^2}{4} \tag{6-9}$$

From the incompressible assumption, these two are equal,

$$2\pi R^2 d(1 - \cos \beta) = d_0 \frac{\pi x_0^2}{4}$$

$$d = d_0 \frac{x_0}{8R^2 (1 - \cos \beta)}$$

$$= d_0 (\frac{x_0}{x})^2 (\frac{1 + \cos \beta}{2})$$

$$= \frac{d_0}{2} (\frac{x_0}{x})^2 (1 + \sqrt{1 - (\frac{x}{2R})^2})$$
(6-10)

By combining eq. 6-6 and eq. 6-10,

$$T = PR(\frac{x}{x_0})^2 / d_0 (1 + \sqrt{1 - (\frac{x}{2R})^2})$$
 (6-11)

Initially, the quantity x is much smaller than R, and the last equation can be approximated as

$$T = PR(\frac{x}{x_0})^2 / 2d_0$$
 (6-12)

But at the end of the experiment, this approximation may introduce a 10% error, and thus it is not recommended.

## 6-4. The Calculation of the Material Functions :

The biaxial extensional stress growth function, as defined by eq. 1-24, is

$$\eta_{\mathbf{b}}^{+}(\hat{\mathbf{\varepsilon}}_{\mathbf{b}}) = \mathbf{T}/\hat{\mathbf{\varepsilon}}_{\mathbf{b}} \tag{6-13}$$

and from eq. 1-25, the steady state value of eq. 6-13 is the biaxial extensional viscosity,  $\eta_b$ . When the strain rate is very small, the stress growth function is expected to be six times the shear stress growth function. So the relationship between  $\eta_b$  and the zero shear viscosity is:

$$\lim_{\dot{\varepsilon}_{b}^{+}} \eta_{b}^{+}(\dot{\varepsilon}_{b}) = 6\eta_{0}$$
 (6-14)

For LDPE,  $\eta_0$  is 71.6 kPas at 130°C, and the low strain rate  $\eta_b$  is expected to be 430 kPas.

## 6-5. Discussion of Experimental Results:

The experimental results are presented in Appendix B. Fig. B-1 shows an empirical relationship between the piston displacement and the strain obtained from earlier experiment results by using eq. 3-12 as the testing model function, where the maximum displacement is 13 cm. An approximation function for this relationship is:

$$X = 3.73 \epsilon_b^2 + 4.43 (1 - \exp(-2 \epsilon_b))$$
 (6-15)

The standard deviation is 0.029. The setpoint table in the program was generated by use of this equation.

Figs. B-2 to B-5 are the strain curves at different strain rates obtained by using eq. 6-15 as the model function. The digital values of all the data points are tabulated in Table B-1. From these curves, it appears that constant rate biaxial extensional flow is generated. The strain rate shown in the upper left corner of each figure was obtained by linear regression analisis of the data, and the standard deviations ranged from 0.0015 ( $\dot{\epsilon}_b$ =0.033/sec) to 0.0077 ( $\dot{\epsilon}_b$ =0.0098). The measured radii of curvature are shown in fig. B-6. It seems that there is no way to predict the radius of curvature at any instant.

In Fig. B-7, the stress growth functions for these experiments are shown. Because of the uncertainty in

measuring the radius of curvature, these are not very accurate. Furthermore, some of the curves are incomplete due to inability to obtain the radius of curvature. Nevertheless, at lower strain rates, the steady state value did approach the expected 430 kPas.

The model function used in "TST1" was obtained by doing nonlinear regression of the data obtained from experiments at constant piston displacement speeds of 0.2, 0.4, and 0.6 cm/sec. These curve, as shown in Fig. B-8, can be approximated as:

$$X = 0.37 \epsilon_b^{3.7} + 21.64 (1-exp(-0.39 \epsilon_b))$$
 (6-16)

with standard deviation of 0.025. The curves given by the above model function are presented in Figs. B-9 to B-11. However, the results are not as good as those presented in Figs. B-2 to B-5. A possible explaination is that the material properties changed due to a temperature decrease.

For both model functions, eq. 6-15 and 6-16, the strain curves obtained are much closer to straight lines than the curves given by eq. 3-15, presented by Rhi-Sausi (6.1).

#### CH. 7 EXPERIENCES DURING APPARATUS MODIFICATION

## 7-1. Designing the Hardware:

The basic requirement for a control system is that it be able to evaluate the controlled variables of the system and adjust these variables by following a model. In a digital system, the variable-evaluation must go through an A/D converter, while the adjustment must be done through a D/A converter. Like other minicomputers, the PET does not have the ability to do either. An interface was therefore developed to meet this requirement.

The first interface designed was based on two IC chips, the AD570 A/D converter and the AD7523 D/A converter. Because neither of these can communicate with the computer, i.e. they cannot be operated directly by the computer, an MC6821 PIA was inserted between the computer and these two chips. This PIA can memorize the data on the data bus as well as on its input ports at the time interval (1  $\mu s$ ) it was selected (that is, the data on the address bus match the address of PIA), and these data can last long enough to be accepted by the computer or to be converted into an analog signal. To control the direction of the piston movement, a relay was connected to the output of the D/A converter and was controlled by the CB2 pin of the PIA. Two operational

amplifiers were used to condition the input signal from the potentiometer that gives the position reading. By using this interface, a program was developed, and the response of the piston was very close to the model, eq. 3-12.

Because of the success of the first interface, a modified circuit was then designed. Two new functions were added: taking pressure readings and controlling the motor A multiplexer, AD7503, with eight channels, drive camera. was employed so that the A/D converter could take data from either the potentiometer or the pressure transducer. operate this multiplexer, another PIA was added. With four pins of one port of the PIA, the computer can select any one of the eight channels. In addition, by connecting the B&c of A/D converter to the EN of the multiplexer, these two chips can be activated simultaneously. An AD558 D/A converter, which can communicate with the computer directly, is used in the new circuit. But because the output level is slightly larger than the input of the servoamplifier, the output is connected to the AD7523 multiplying D/A converter, so that the output level can be adjusted by the computer; addition, because the AD7523 is connected in the bipolar operation mode, the direction of piston movement can be controlled by assiging a proper number to the multiplying D/A converter. The operation of AD7523 is the same as in the first circuit, through a PIA. The pressure transducer is connected to a signal conditioning module 2B31, which has three basic functions : amplifying, filtering, and transducer exciting. Another operational amplifier is connected to the output of the 2B31 to adjust the analog signal so that its corresponding digital signal is equal to the pressure reading in units of 10 Pa. The interface circuit is described in chapter 4 in more detail.

## 7-2. Designing the Software:

The most straightforward way to control the piston movement is to take a reading, compute the required output voltage, and send out the signal. However, this procedure is too slow to match the speed of the piston. A more practical method is table-look-up. The output values corresponding to position readings are prepared as a table and stored in the memory of the computer before the start of an experiment. In the course of controlling, the computer only has to take the reading and output a voltage referred to the table in the memory, and the computing time is saved. This method proved to be effective and was adopted as the principle of software design.

In the earlier programs, the table was computed in the first part of the program, which is a time-consumming process. Because the table is always the same for every experiment, it is inefficient to compute the table every time; therefore in the later program the table is saved on cassette tape and loaded into memory before the experiment begins. But later this loading process was found still to

be slow, and finally, the table is inserted in the program; although it is very tedious to type 512 numbers, the loading time is greatly shortened.

In the beginning, the model used in preparing the table was eq. 3-12. But after several experiments, the strain curve obtained was found not to have a constant strain rate. A new table of position against strain was then prepared and adopted in the later experiments, and the data obtained show that these are constant strain rate experiments.

In the previous program, the maximum piston displacement was set at 13 cm. To attain higher strain, this displacement is set to 17 cm. A program, TEST, which is for generating the empirical correlation, was developed. The other program, TST1, was revised from the older program for obtaining experiment data. These two programs are described in section 4-3.

## 7-3. Development of Experimental Techniques:

The experimental procedure at first followed that developed by Rhi-Sausi, except for the control system operation. However, it was soon found that his method of photographing was not efficient. It takes time to have the cinema film developed, and the frame speed is not synchronized with the motor drive camera. To improve this, a

45 ° mirror was mounted on the clamping ring, so that both the front view and the side view can be photographed on the same frame. The data-analyzing procedure was revised also; insteaded of using the film analyzer, a projector was used, which provided a wider field of vision for locating the marks on the bubble surface. The experimental procedures are described in chapter 5.

# 7-4. Operation of the Extensiometer:

## 7-4-1. Photography:

The pictures are taken at an aperture of f32 and a speed of 1/30 s using ASA 400 film to have a deep field of focus. The films are developed by using Microdol-X with 12 minute developing time; thus higher contrast images are obtained.

To obtain clear photos the heating medium should be filtered when it begins turning cloudy. The best filtering method is vaccum filtering with #42 filter paper. However, because of the high viscosity of the oil, it takes 2 days to filter all 4 liters of oil.

## 7-4-2. Pressure balancing before an experiment:

Although there is a tube for balancing the oil pressure, it does not work efficiently, because the rate of

thermal expansion is faster than the oil can flow through the tube. The overflow vent on the top of the fixed chamber is used to drain the extra volume of oil. The criterion for balanced pressure is the flatness of the sample disk.

#### CH. 8 SUMMARY AND RECOMMENDATIONS

#### 8-1. Summary:

## 8-1-1. The hardware development:

An electronic circuit was designed and assembled, which has the abilities of two channel A/D conversion, multiplying D/A conversion and D/A conversion. Through this circuit, a PET minicomputer can control the motion of the piston, take pressure readings and take pictures periodically.

### 8-1-2. The software development:

Two different programs were developed. The program TEST is for controlling the piston moving at a constant speed to obtain an empirical relationship between the position of the piston and the strain. The other program, TST1, controls the piston moving according to the empirical relationship, to generate a constant strain rate biaxial extensional flow. Both programs are able to take pictures as well as pressure readings besides controlling piston movement.

#### 8-1-3. The development of experiment technique:

The technique described in Rhi-Sausi's Ph.D. Thesis was revised. the original analog control system was replaced by a digital system, featuring automated operation. By adding a 45° mirror, the photographic data are easier to analyze. The analyzing technique was also modified by the use of a projector, which makes the analyzing less difficult.

## 8-1-4. Demonstration of the extensiometer :

Several experiments were carried out by testing LDPE (CIL 560) at 130°C. The strain curves obtained were close to a constant strain rate curve. However, the highest strain rate is only 0.06 per sec, and the highest strain achieved is 1.85.

## 8-2. Recommendations:

## 8-2-1. Improvement of the extensiometer:

- (1) To improve the present temperature nonuniformity problem, oil stirring is required as well as better insulation of the chambers.
- (2) To attain a higher strain rate, the gear ratio should be reduced to increase the maximum piston speed.

(3) To achieve higher strain, the shaft length should be increased.

## 8-2-2. Improvement of the experiment technique:

- (1) To extend the validity of this apparatus to a variety of materials, the sample preparation method must be improved. The present method, compression molding, does not mix the pellets during the preparation of the sample disk; therefore the boundaries between pellets are not eliminated completely, and this weakness causes the bubble to puncture during the inflation process. Perhaps a better method is injection molding.
- (2) When the experimental results are reproducible, an empirical relationship of radii of curvature and time may be obtained. As mentioned in Rhi-Sausi's thesis, this relation along with a thickness empirical function and the pressure reading make it possible to obtain the biaxial extensional stress growth function without analyzing photographs.
- (3) A better way to generate constant strain rate extesional flow is to control the piston movement by direct measurement of the strain, which is determined by measuring the bubble thickness at the pole. The thickness measurement might be done by measuring the intensity of a sonic wave passing through the bubble shell.

#### REFERENCES

- 1.1. J.M. Dealy, Rheometers for Molten Plastics , van Nostrand-Reinhold, N.Y., 1982
- 1.2. R.B. Bird, R.C. Armstrong, and O. Hassager, Dynamics of Polymeric Liquids: Fluid Mechanics, v. 1., John Wiley, N.Y., 1977
- 1.3. S. Middleman, Fundamentals of Polymer Processing, Ch. 1, McGraw-Hill, N.Y., 1977
- 2.1. L.S. Thomas and K.J. Cleereman, S.P.E. J., 28, 61 (April 1972)
- 2.2. R. Farber, Research Proposal, Chem. Eng. Dept., McGill Univ., 1974
- 2.3. J. Meissner, T. Raible and S.E. Stephenson, Paper presented to Society of Rheology, Boston, Nov. 1979
- 2.4. J.F. Stevenson, Personal communication to J.M. Dealy
- 2.5. Sh. Chatraei, and C.W. Macosco, J. Rheol. in press (1981)
- 2.6. L.R.G. Treloar, Trans. Inst. Rubber Ind., 19 , 201 (1944)
- 2.7. C.D. Denson and R.J. Gallo, Polym. Eng. Sci., 11,174 (1971)
- 2.8. D.D. Joye, W. Poehlein and C.D. Denson, Trans. Soc. Rheol., 16,421 (1972)
- 2.9. J.M. Maerker and W.R. Schowalter, Rheol. Acta, 13,627 (1974)
- 2.10. A.J. De Vries and C Bonnebat, Polym. Eng. Sci., 16,93 (1976)
- 2.11. K.C. Hoover and R.W. Tock, Polym. Eng. Sci., 16,82 (1976)
- 2.12. C.D. Denson and D.C. Hylton, Proc. VII Congr. Rheol., Gothenburg, 1976, p. 386
- 2.13. J. Rhi-Sausi and J.M. Dealv, Polym. Eng. Sci., 21,227 (March 1981)

- 2.14. C.J.S. Petrie, Elongational Flow , p. 91, Pitman, London, 1979
- 3.1. J. Rhi-Sausi, Ph.D. Thesis, Ch.3-C, Chem. Eng. Dept., McGill Univ., May, 1979
- 4.1. Y.C. Chao, H.P. Huang, Process Control (in Chinese), v. 2, Ch.14,
- 4.2. C.L. Smith, <u>Digital Computer Process Control</u>, Intext Educational publishers, 1972
- 4.3. R.P. Hunter, Automated Process Control Systems, Prentice Hall, NJ, 1979
- 4.4. Data Acquisition Components and Subsystems Catalog, Analog Devices Inc, Norwood, MA, 1980
- 4.5. MCS 6500 Microcomputer Family Hardware Manual, MOS Technology Inc., Norristown, PA, 1976
- 5.1. CBM 2001 Professional Computer User Manual, Commodore Bussiness Machines Inc., Santa Clara, CA, 1979
- 5.2. J. Rhi-Sausi, Ph.D. Thesis, Ch.3-D, Chem. Eng. Dept., McGill Univ., May 1979
- 6.1. J. Rhi-Sausi, Ph.D. Thesis, Ch.4

# APPENDIX A:

PROGRAMS AND CIRCUIT DIAGRAM

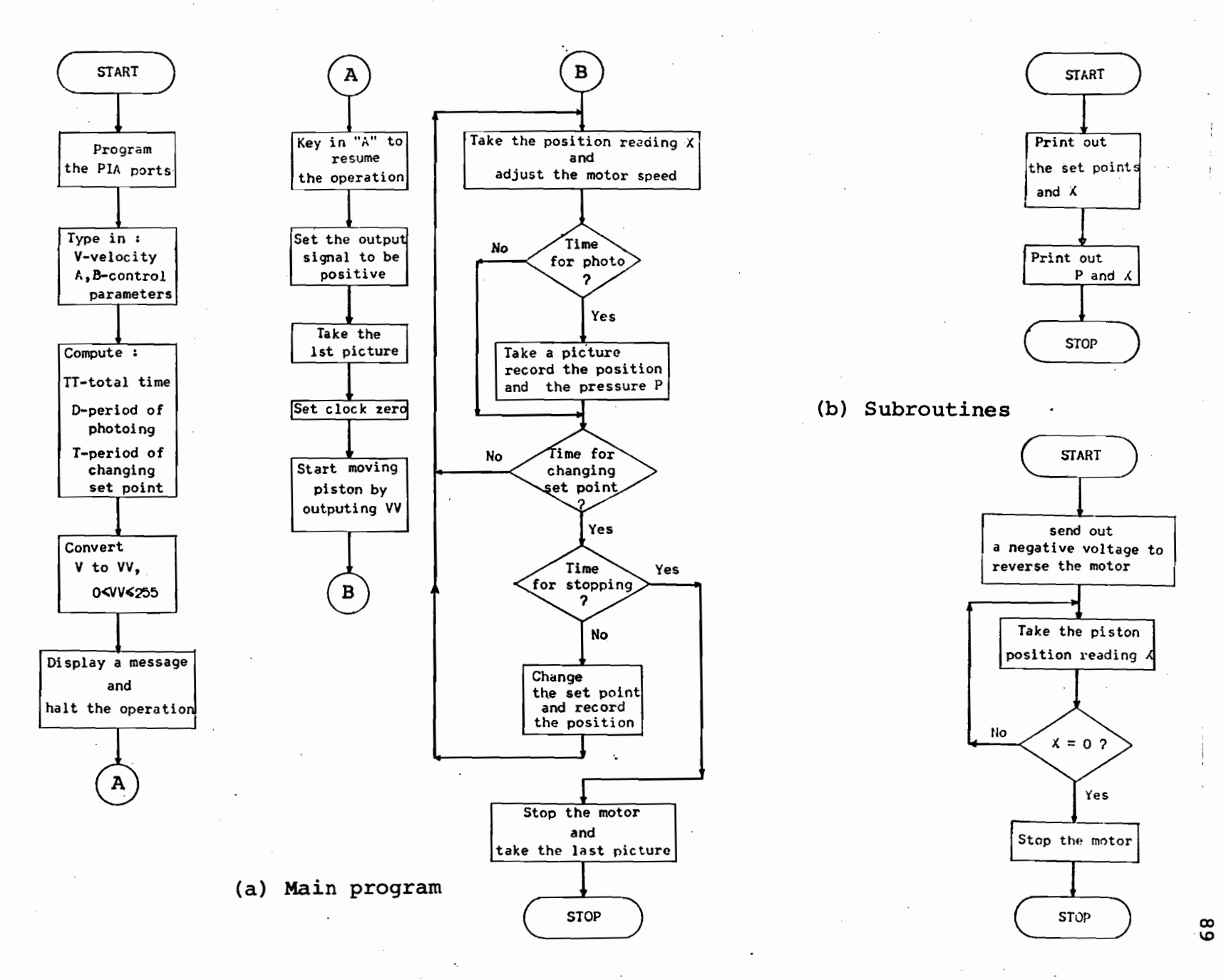


Fig. A-1 Flowchart of the program "TEST"

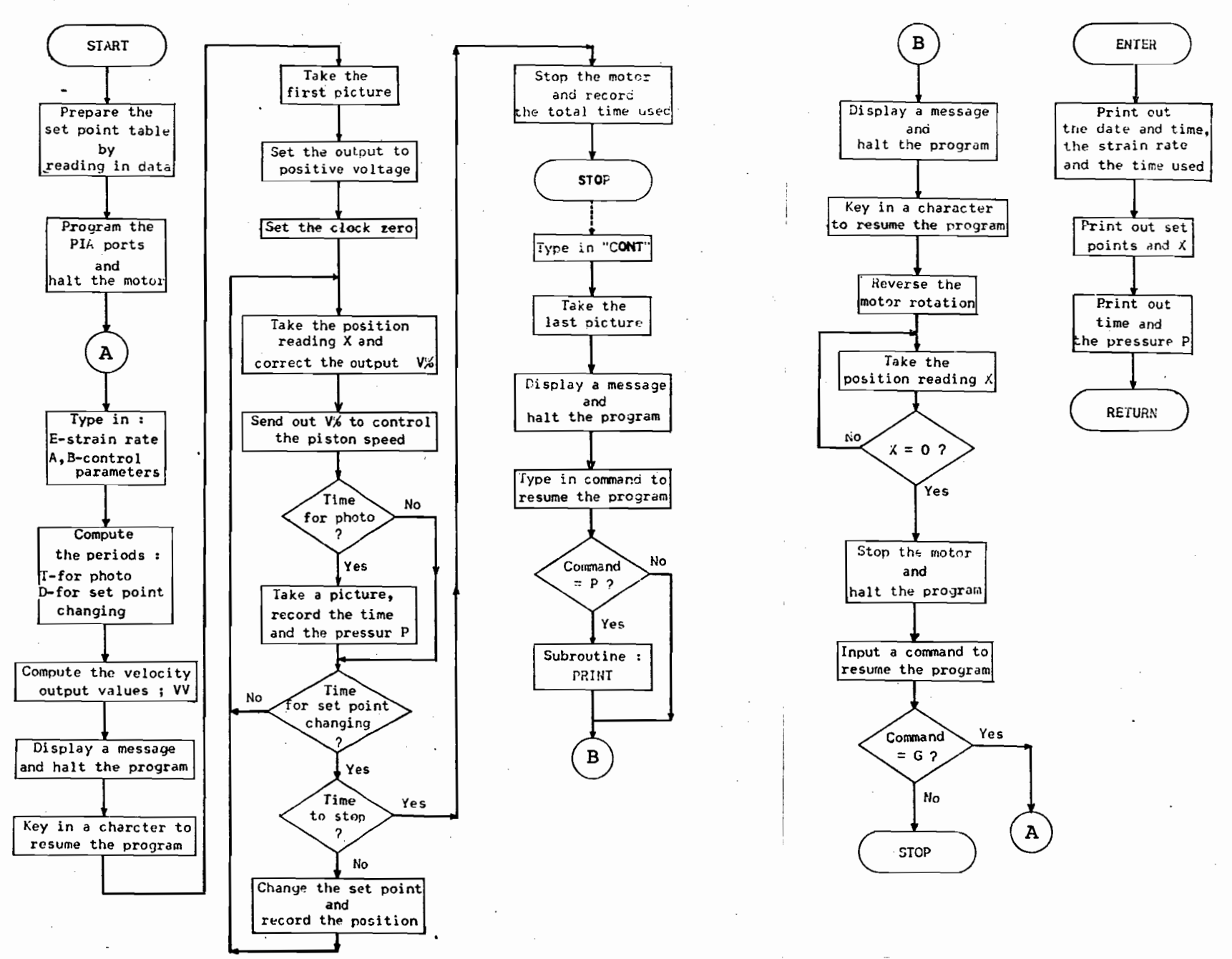


Fig. A-2 Flowchart of the program "TST1"

```
G DIST(40),XX(255),PX(40)
19 REP -----INITIATION
28 POKE29673,0:POKE28672,0:POKE28673,52
21 PGKE28675,0:POKE28674,248:POKE28675,52:POKE28674,136
22 POKE28679,0:POKE28678,255:POKE28679,52:POKE28678,128
23 POKE28677,52:PCKE28680,0
25 INPUT"SPECIFY V.A.B";V.A.B
29 REM -----TIME SCHEDULING-----
30 MX=17
35 TT=MX/V*60
40 D=TT/30
45 T=TT/255
50 VV=8*V
60 PRINT"™ READY TO GO, PRESS A"
70 EMPUTOS
79 REM ------CONTROLLING-----
30 POKE28678,90
98 FORI=17010:POKE28674,128:WEXTI:K=1:POKE28674,16:PX(1)=PEEK(28672)
188 TI$="000000"
110 POKE28680,VV
120 FORJ=1T0255
140 IFTIKD*KTHEN160
150 POKE28674,128:POKE28674,16:K=K+1:T(K)=XX:PX(K)=PEEK(28672)
:60 IFTICT*JTHEN130
:70 X%(J)=X%
180 MEXTI
198 FORI=17010:POKE28674,128:NEXTI:K=K+1:T(K)=TI/4
195 POKE28674,136
200 STOP
218 FORI=1T0255:PRINTI,X%(I),I-X%(I):NEXTI
220 FORI=1TOK:PRINTI;T(I)/15,P%(I)*10:NEXTI
230 STOP
240 INPUT"IREADY TO RESET, PRESS G";C$
249 REM ------RESETTING-----
250 POKE28678,255:POKE28680,80
260 POKE28674,136:POKE28674,8:IFPEEK(28672))000T0250
270 POKE28680J0:POKE28678J128
280 STOP
```

Fig. A-3 The program "TEST"

```
400 POKS28678,255:POKE28680,80
                                                                                  410 POKE28674,136:POKE28674,8
                                                                                  420 IFPEEK(28672)=0G0T0440
                                                                                  430 GOTO410
5 PRINT"CLOADING TABLE"
                                                                                  440 POKE28680.0:POKE28678,128:POKE28674,136
18 DIMXX(255),T(255),V(255),XXX(255),VV(255),PX(255),X(255)
28 111-17
                                                                                  450 PRINT"TYPE Q TO QUIT; TYPE G TO NEXT RUN"
                                                                                  460 IMPUTOS
30 SM=2.038323161
                                                                                  470 IFC$="G"THEN180
40 FORI=0T0255
                                                                                  480 PRINT"GOOD-BYE"
50 READXX(I),X(I)
                                                                                  490 STOP
SO MEXTI
70 INPUT"DATE";D$
                                                                                  500 OPEN1,4,0:OPEN2,4,2:OPEN3,4,1
88 STOP
                                                                                  501 PRINT#1, "DATE=": D$+", "+T$
                                                                                  503 PRINT#1, "STRAIN RATE=";E; "/SEC"
159 POKE28679,0:POKE28678,255:POKE28679,52:POKE28677,52
                                                                                  504 PRINT#1, "MRX DISPLACEMENT=";MX;"CM"
160 POKE28673,0:POKE28672,0:POKE28673,52
                                                                                  505 PRINT#1, "TIME ELAPSED=";TT; "SEC"
170 POKE28675,0:POKE28674,248:POKE28675,52:POKE28674,136
                                                                                  506 PRINT#2, " 999.99 999 999
71 INPUT"TIME";T$
                                                                                  507 PRINT#1
171 PROGETIMENTS
172 PRINT"CREADY"
175 POKE28680,8:POKE28678,90
100 PRINT"WHAT IS THE STRAIN RATE ?
185 INPUTE
                                                                                  508 FORN=0T0255
                                                                                  509 TM=SM/E*N/255
                                                                                  510 PRINT#3, TM, XX(N), XXX(N); XXX(N)-XX(N)
                                                                                  5:5 PRINTTM;XX(N);XXX(N)
186 INPUT"SPECIFY A,B";A,B
                                                                                  520 NEXTN
187 K1=E*8
                                                                                  525 PRINT#1
191 PRINT""
                                                                                  530 PRINT#2, "99
198 T=8M/E/30*60
                                                                                  532 FORN=1TOK
199 D=SM/E/255*60
                                                                                  535 PRINT#3,N,T(N),P%(N)
200 FORI=1T0255
                                                                                  540 PRINTH; T(N); PX(N)
205 VV(I)=A*(X(I)-X(I-1))/D*60
                                                                                  550 NEXTN
218 IFV>250THENV=250
230 PRINTVV(I)
                                                                                  560 CLOSE:
                                                                                  Sie GLüstz
240 NEXTI
                                                                                  580 CLOSE3
255 PRINT"DREADY"
256 PRINT"TO INITIATE THE CONTROL, TOUCH A"
                                                                                  590 RETURN
                                                                                  600 FORI=0T0255
257 INPUTC$
                                                                                  610 PRINTI:XX(I):XXX(I):XXX(I)-XX(I)
258 FORN=1T010:POKE28674,16:NEXTN:K=1:PX(K)=PEEK(28672):POKE28674,136
259 PRINT"DONTROLLING THE EXPERIMENT"
                                                                                  620 NEXTI
                                                                                  630 FORN=1TOK
264 PRINT
265 PRINT"
                                                                                  640 PRINTN; T(N); PX(N)
               DO NOT INTERRUPT "
266 POKE28678,90
                                                                                  650 NEXTN
                                                                                  660 STOP
269 TI$="000000"
                                                                                  700 DATA0,0,1,.0715832,2,.1428676,3,.2138559,4,.284551,5,.3549557
270 FORJ=1T0255
280 POKE28674,136:POKE28674,8:X%=PEEK(28672)
                                                                                  701 DATA6,.4250729,7,.4949056,8,.5644567,9,.6337292,10,.7027261
                                                                                      DATA11,.7714504,12,.8399051,13,.9080933,14,.976018,15,1.0436823
290 VX=INT(VV(J)+B*(XX(J)-XX)):IFVX>250THENVX=250
                                                                                 703 DATA16,1.1110892,17,1.1782418,18,1.2451431,19,1.3117964,20,1.3782046
300 POKE28680, V%
305 IFTICT*KTHEN310
                                                                                 704 DATA21,1.4443708,22,1.5102982,23,1.5759899,24,1.6414489,25,1.7066784
705 DATA26,1.7716815,27,1.8364613,28,1.9010209,29,1.9653635,30,2.0294922
306 POKE28674,144:POKE28674,16
                                                                                      DATA31,2.0934101,32,2.1571203,33,2.220626,34,2.2839303,35,2.3470364
397 K≠K+1
                                                                                 707 DATH36,2.4099473,37,2.4726663,38,2.53519964,38,2.5975409,39,2.65978838
308 P%(K)=PEEK(28672)
                                                                                 703 DATA40,2.7216852,41,2.7834914,42,2.8451245,43,2.9065875,44,2.9678838
709 DATA45,3.0290163,46,3.0899883,47,3.1508029,48,3.2114633,49,3.2719725
309 T(K)=TI/60
310 IFTICD*JTHEN305
                                                                                  710 DATA49,3.3323338,50,3.3925502,51/3.452625,52,3.5125613,53,3.5723621
320 XXX(J)=XX
                                                                                  711 DATA54,3.6320307,55,3.6915703,56,3.7509838,57,3.8102746,58,3.8694457
330 NEXTJ
                                                                                  712 DATA53,3,9285003,59,3,9874415,60,4,0462724,61,4,1049963,62,4,1636162
335 POKE28680,0:POKE28678,128:TT=TI/60:POKE28674,136
                                                                                  713 DATA63,4.2221352,64,4.2805566,65,4.3388835,65,4.3971189,66,4.4552661
                                                                                  714 DATR67,4.5133282,68,4.5713082,69,4.6292094,70,4.6870349,71,4.7447877
341 FORN=1T010:POKE28674,16:NEXTN:K=K+1:PM(K)=PEEK(28672):POKE28674,136
                                                                                  715 DATA72,4.8024711,72,4.8600882,73,4.917642,74,4.9751358,75,5.0325726
342 PRINT"TEND OF EXPERIMENT"
                                                                                  716 DATA76.5.0899556,77,5.142879,78,5.2045726,78,5.2618129.79,5.3190118
350 PRINT"TYPE R TO RESET; TYPE P TO PRINT"
                                                                                 717 DATAS0,5.376172,81,5.4332982,82,5.4903918,83,5.5474567,84,5.6044957
718 DATAGE,5.6615122,85,5.7185092,86,5.7754897,87,5.832457,88,5.8394141
360 INPUTC$
370 IFC$="P"THENGOSUB500
                                                                                  719 DATA89,5.9463642,90.6.0033103,90,6.0602556,91,6.1172031.92,6.174156
380 PRINT"RESET THE EQUIPMENT; IF ALL SET, TYPE Y"
                                                                                 720 DATA93,6.2311174,94.6.2880903,95,6.3450779,96,6.40200833,96,6.4591096
390 INPUTO≸
```

Fig. A-4. The Program "TST1" (Cont'd)

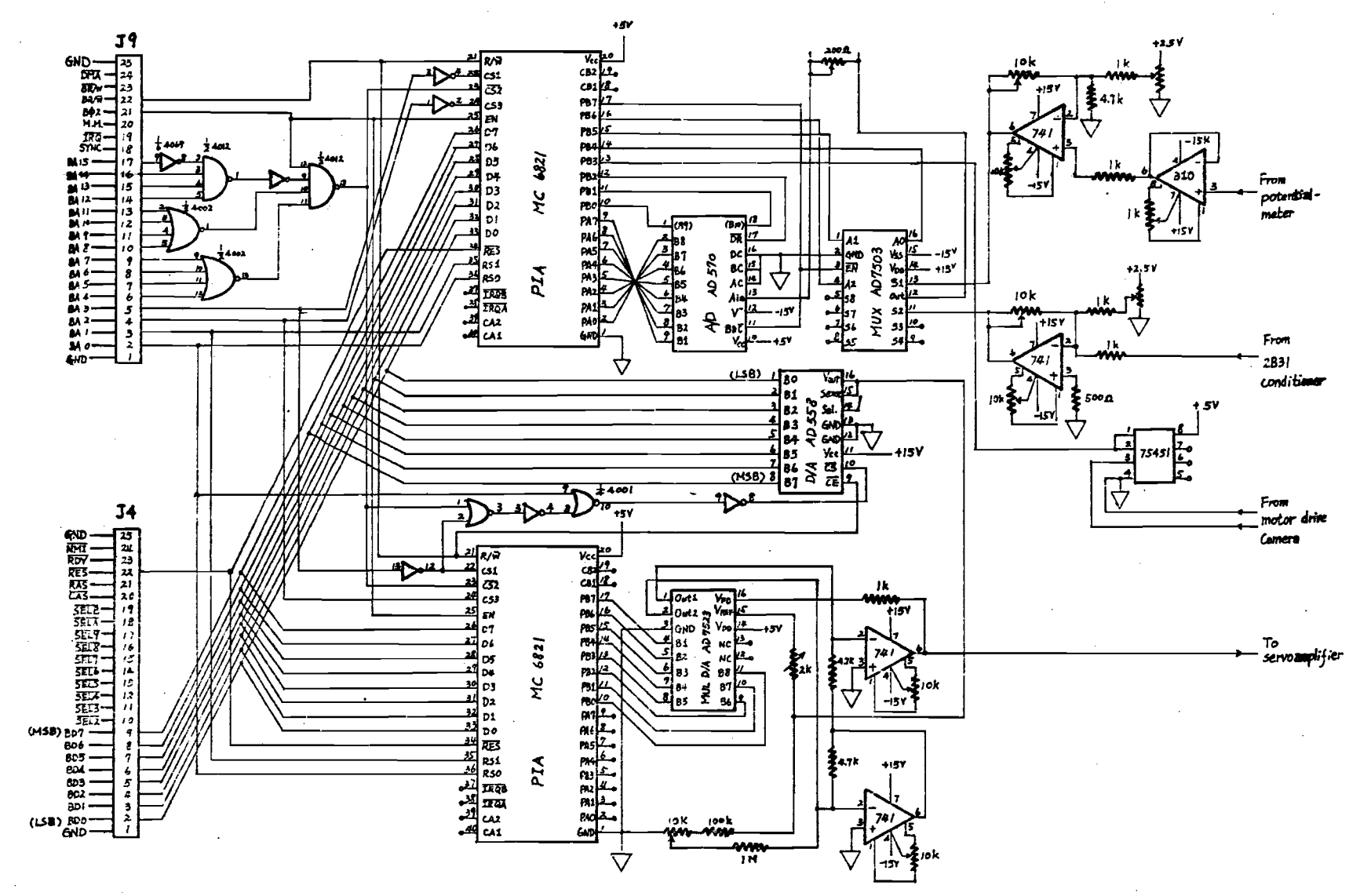


Fig. A-5 The circuit diagram of the interface

APPENDIX B:

EXPERIMENT RESULTS

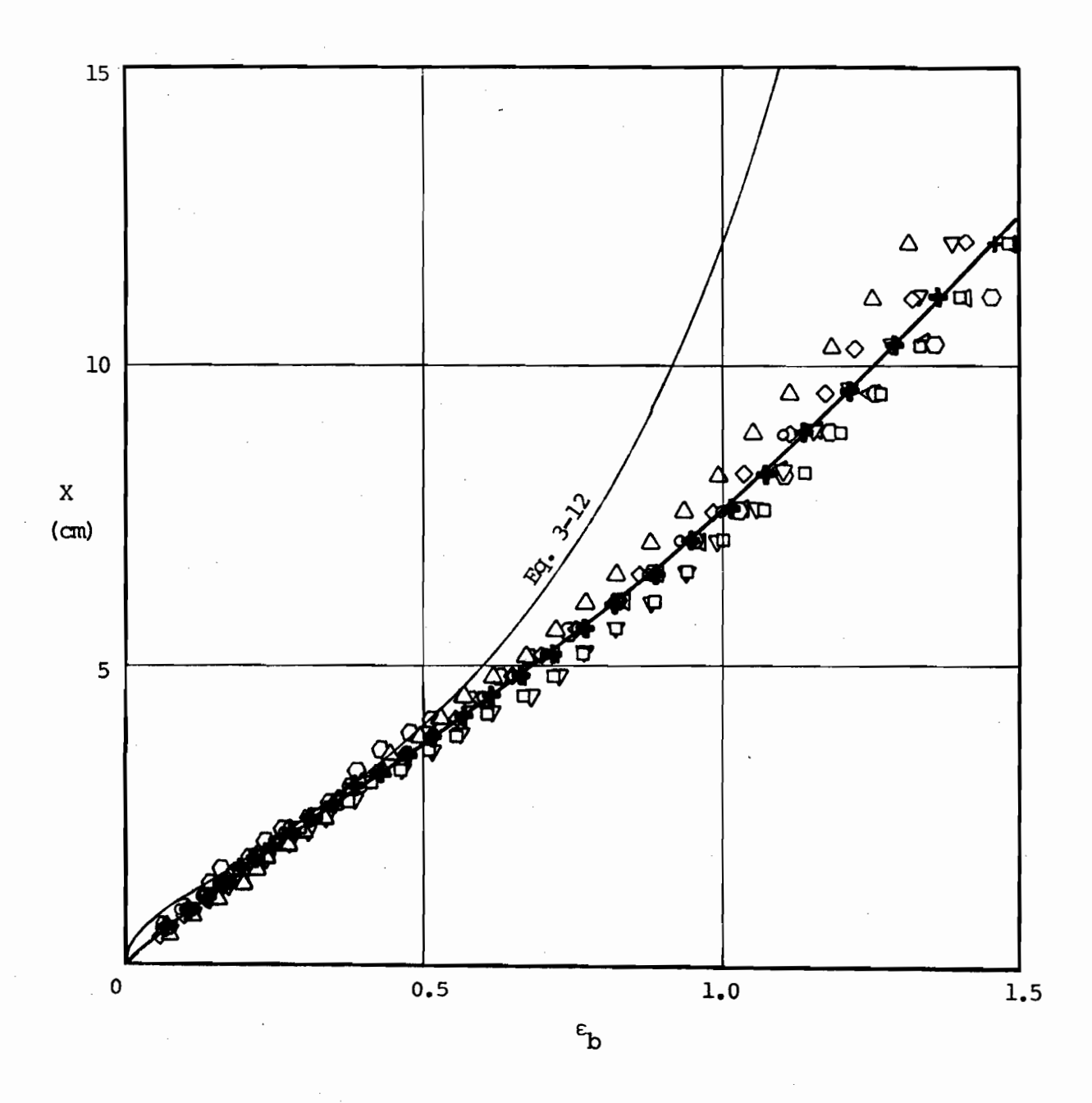


Fig. B-1. The Empirical Relationship of X and strain  $(X \le 13 \text{ cm})$ 

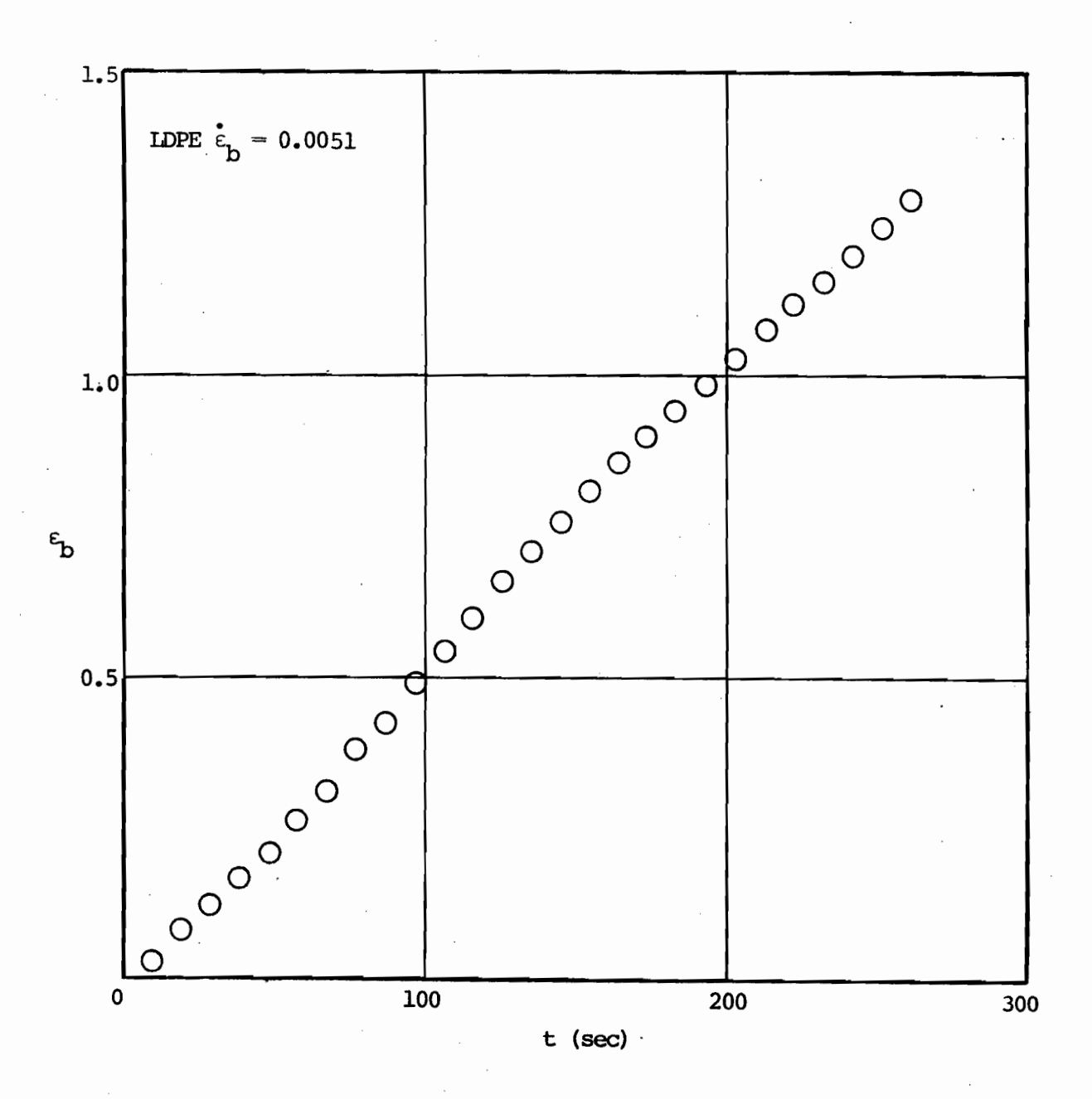


Fig. B-2. Strain Curve (set strain rate: 0.005 /sec)

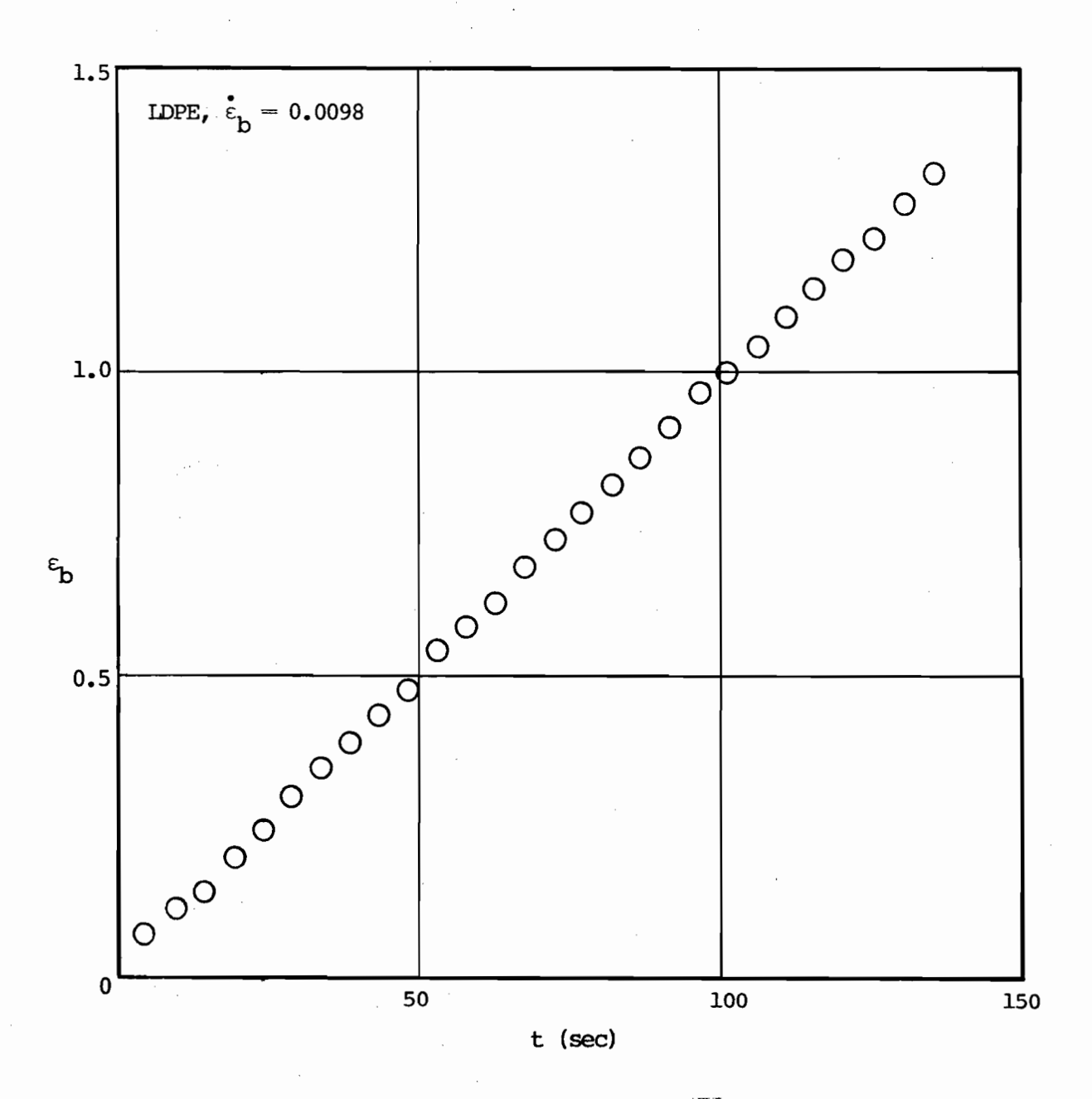


Fig. B-3. Strain Curve (set strain rate: 0.01 /sec)

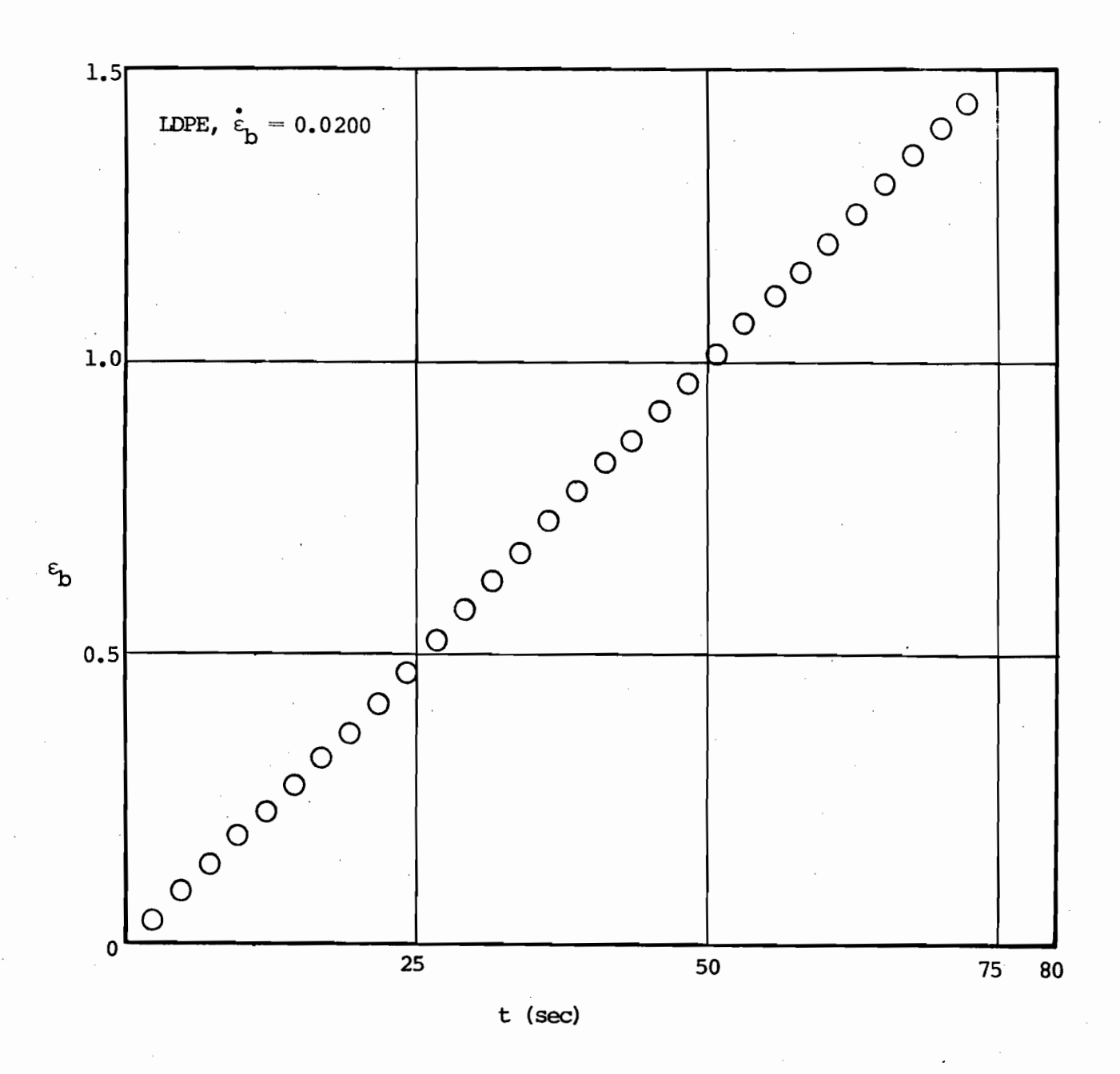


Fig. B-4. Strain Curve (set strain rate: 0.02 /sec)

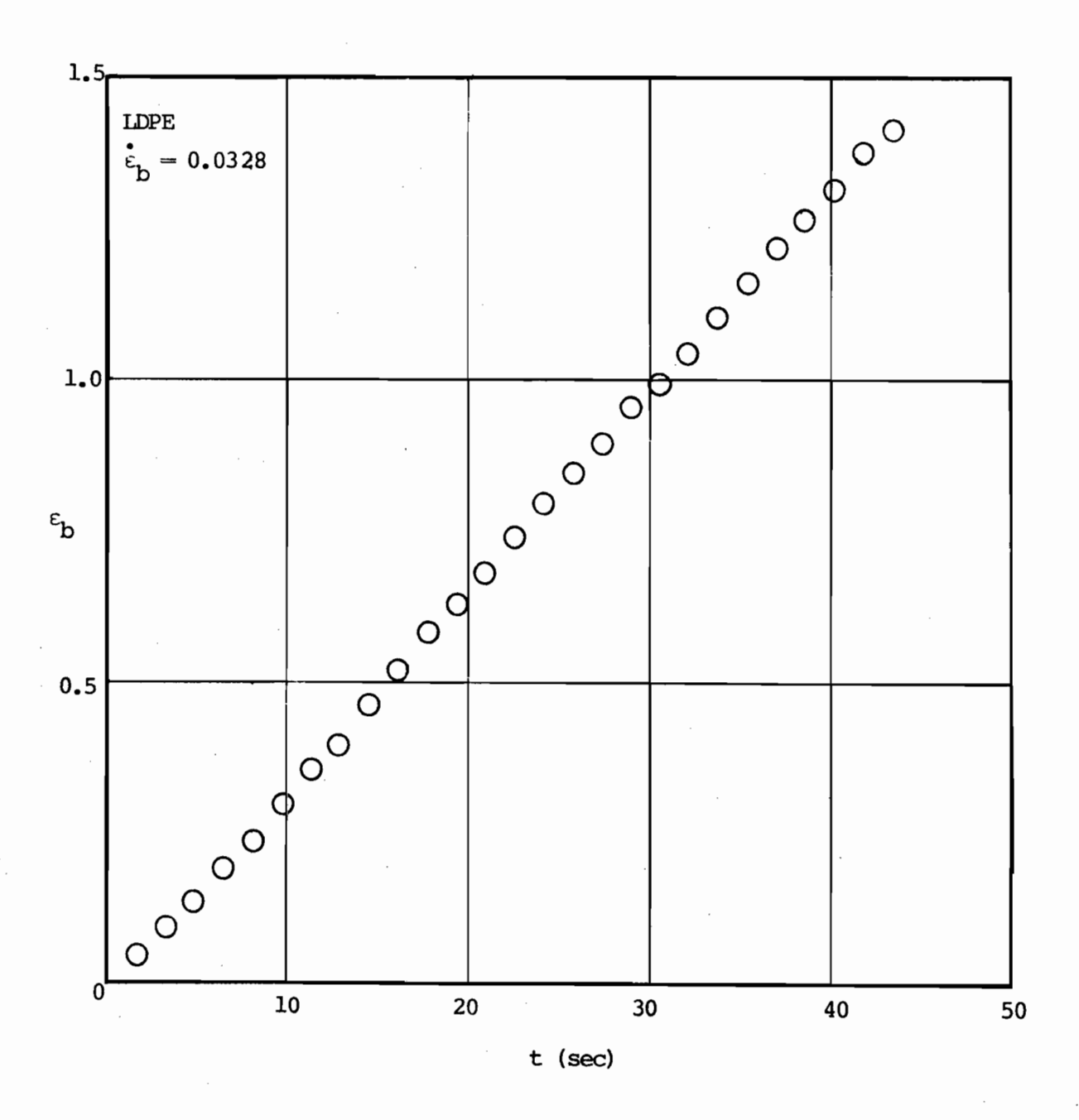


Fig. B-5. Strain Curve (set strain rate: 0.03 /sec)

55-83
11
E E E
2746H0

Œ.

STRINGS.

STREETS

(0)

H

(S) (B)

STRBIN RATE

Œ L	
STRESS,	$\begin{array}{c} ++++OOOOOOOOOOOOOOOOOOOOOOOOOOOOOOOOO$
STRAIN	$\begin{array}{c} a \\ a \\ b \\ c \\ c$
7,45,5	

44000

 $\frac{1}{4}$ 

3861

0000 4000

(a) For Fig. B-2

(b) For Fig. B-3

σ: σ:

Table B-1. Expriment Results

030 031
н
10 Fr 60 60
7. 10. 10. 10. 10. 10. 10. 10. 10. 10. 10
100

1 ! 1 i

00

1, i

OF THE PERSON OF

Œ ŭ.	
STRESS,	& C & & & C C C C C C C C C C C C C C C
STRHIN	$\begin{array}{c} \alpha \alpha$
TIME, S	$\frac{1}{\sqrt{4}\sqrt{9}} \frac{1}{\sqrt{9}} \frac{1}{$

(c) For Fig. B-4

(d) For Fig. B-5

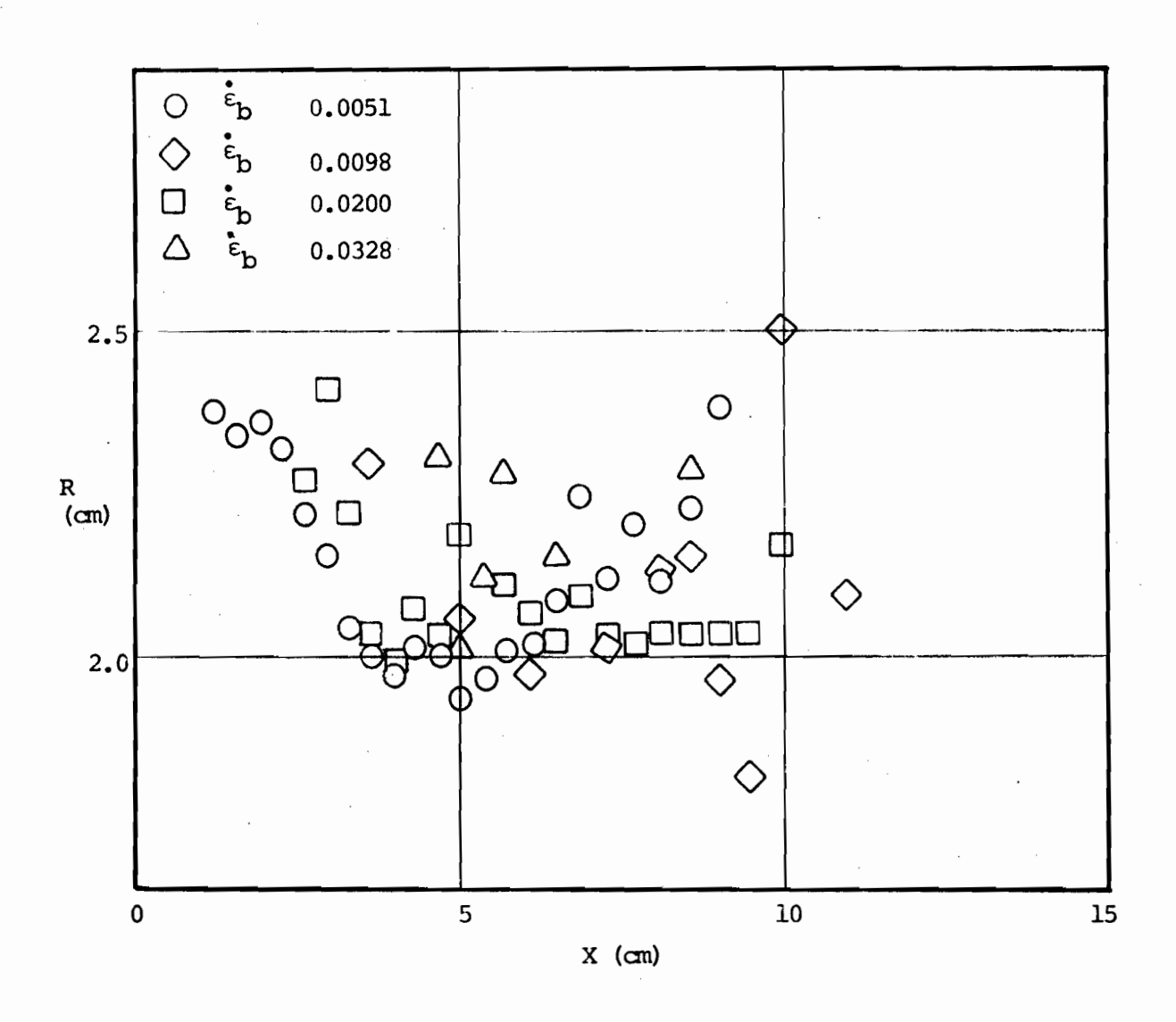


Fig. B-6. The Relationship between Radius of Curvature

and Piston Displacement

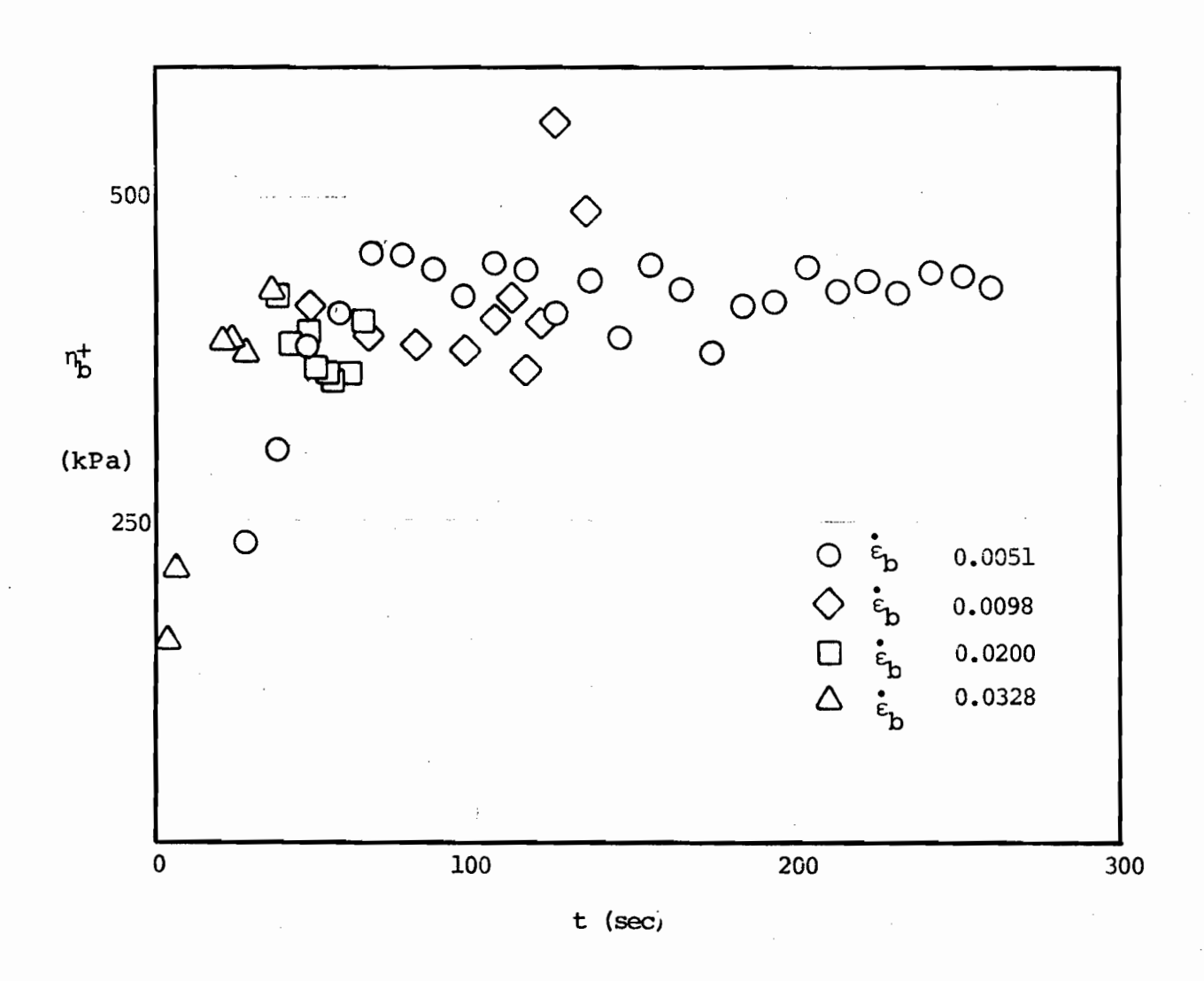


Fig. B-7. The Stress Growth Function

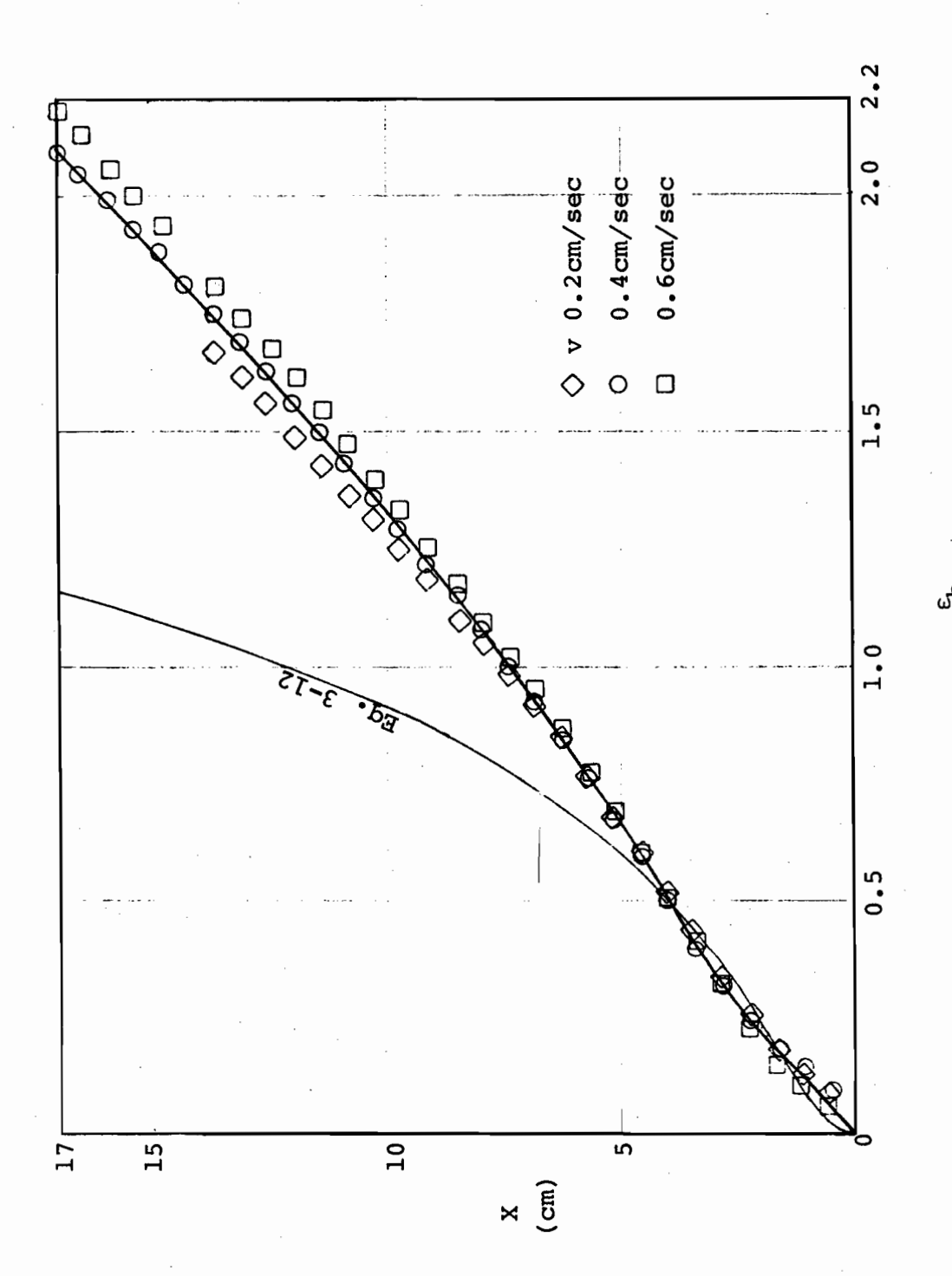


Fig. B-8. The Empirical Relationship of X and Strain (X ≤ 17 cm)

77 (C) (C) (C) (C)	& &	, , , , , , , , , , , , , , , , , , ,	, , , , , , , , , , , , , , , , , , ,	0
(O) (II) (E) (E) (E) (E) (E) (E) (E) (E) (E) (E	ಇಪ್ಪುಗಳು ಪ್ಪ ಗಳನ್ನು ಗಳನ್ನ	4 W W W W W W W W W W W W W W W W W W W	ស្រែកក្នុកស្រុ ស្រែកក្នុកស្រុក ស្រុកក្នុកស្រុកប្	നെ എന്നുന്നുന്ന സംഗത്തന്ന് അന്സ്

Fig. B-9. Strain Curve and the Experiment Result (set  $\hat{\epsilon}_{b}$ : 0.01/sec)

හිය	STREIN	######################################
STRAIN ABTE	00 10 20 14 14	ရေးကြည်း ကို ရေးသည် မေရာက် မေရာက် မေရာက် မေရာက် မေရာက မေရာက် မေရာက် မေရာက

Fig. B-10. Strain Curve and the Experiment Result (set  $\epsilon_{\rm b}$ : 0.04/sec)

0.06/sec) (set Strain Curve and the Experiment Result Fig. B-11.

APPENDIX C:

GLOSSARY OF TERMS

## GLOSSARY OF TERMS

Actuator: A transducer whose output is mechanical motion.

- Address: A unique identification code assigned to each memory location and device with which a digital computer must communicate.
- Analog: Representation of naturally occurring system variables by a unique set of values having neglegible separation between adjacent values.
- A/D Converter: A device which accepts an analog quantity at its input and produces a binary code at the output for each value of analog input.
- Bit: The abbriviation of <u>Binary Digit</u>, the smallest unit of digital identification. (0 or 1)
- Bus: A set of electrical conductors which are used to transmit information from one place to another, both internally and between the computer and external devices.
- Byte: A group of bits that are to be interpreted together to decode the information they represent.

- Data: Information which is generated, processed, and transfered by a digital computer.
- Derivative Control: A control mode which only provides an output that is related to the time rate-of-change of the difference between the instantaneous value of the process variable and its setpoint.
- Digital: Representation of naturally occurring system variables by a limited number of discrete values having a discrete separation between adjacent values with no interim values possible.
- D/A Converter: A device which accepts discrete binary codes at its input, and produces a unique analog signal at its output for each discrete input value.
- Direct Digital Control: A control strategy in which a process control digital computer is in complete control of the process directly.
- Integral Control: A control mode which only provides an output that is related to the time integral of the difference between the instantaneous value of the process variable and its setpoint.
- Least Significant Bit (LSP): The bit which is closest to

the binary point in the integer portion of a binary value.

- Machine Language Programming: The process of writing a digital computer program directly in the binary codes and addresses that the computer requires in order to execute the program.
- Most Significant Bit (MSB): The bit which is furtherest from the binary point in the integer portion of a binary value.
- Multiplex: The sharing of specific devices, circuits, or wires for many mutually independent purposes.
- Offset: A measurable output from a circuit or device when a zero signal is applied to its input.
- Operational Amplifier: A category of electronic amplifier for performingmathematics functions as integral parts of analog computers.
- PEEK: A BASIC instruction that returns the values stored in the location specified.
- Peripheral: Hardware that connects to a digital computer and communicates with the computer.

- POKE: A BASIC instruction that loads the specified value into the specified location.
- Program: A series of appropriately coded instructions which sequentially control the operation and data manipulation executed by a digital computer.
- Proportional Control: A control mode in which the output is a linearly related function of the difference between the instantaneous value of the process variable and its setpoint.
- PID Controller: A controller which provides an output that is a linear combination of proportional control, integral control, and derivative control.
- Relay: An electromechanical device having two independent circuits. The activating circuit is normally an electromagnetic coil which magnetically operates sets of contacts which are parts of other electrically isolated circuits.
- Resolution: A statement of the largest incremental change in the input which will produce no detectable change in the output.
- Sample-and-Hold: An electronic circuit which performs the

## functions of

- (1) Sampling: in this mode the output is the same as the input.
- (2) Hold: in this mode its input is disconnected from the signal it was sampling and its output remains at the value it was at the instant the input was disconnected.
- Supervisory Control: A control strategy where the process control computer performs system control calculations and provides its output to the setpoint inputs of conventional analog controllers.
- Transducer: A hardware piece of equipment which converts variable information from one energy system to another energy system.